Measuring Muon Lifetime and Muon velocity

Uzair Abdul Latif
Senior Year Project Report
Supervisor: Dr. Imran Younas
Department of Physics
LUMS School of Science and Engineering

Wednesday, April, 30, 2014

Abstract

This project report starts by giving a theoretical backround of cosmic rays and muons as observed on earth. There are two segments to this project. The first segment is about how the lifetime of the cosmic ray Muons was measured using plastic scintillators, photomultiplier tubes, NIM standard module and a multi-channel analyser. The second segment talks about how the Muon velocity was measured using a very similar setup to that of the lifetime experiment. A Monte Carlo simulation was also carried out in order to determine the average distance travelled between the detectors in the velocity measurement experiment. The value of the lifetime obtained from the experiment was $\tau = 2.30 \pm 0.09 \mu s$ and the value of velocity of the muon obtained was $< v_\mu >= (3.2 \pm 0.1_{sys} \pm 0.3_{stat}) \times 10^8 ms^{-1}$.

Contents

Chapter 1

Introduction to Cosmic Rays

Most of the content of this section has been taken from the book of Todor Stanev's book "*High Energy Cosmic Rays*" [1].

1.1 Cosmic Rays Origins

Cosmic ray particles are charged particles of interstellar origin. Cosmic rays, on a basic level, are defined as those particles which are able to reach earth from interstellar space. The flux of Hydrogen and Helium nuclei dominates the cosmic ray spectra in the GeV energy range. Then there is the steady flux of electrons followed by rare entries of anti-matter particles which include positrons and anti-protons.

Cosmic ray particles basically originate from nuclear fusion reactions occurring inside stars. Some of these reactions are:

$$
\begin{gathered}
4H^{+} \rightarrow He + \gamma \\
p + p \rightarrow H_2 + e^{+} + \upsilon_e \\
H^2 + p \rightarrow He_3 + \gamma \\
He_3 + He_3 \rightarrow He_4 + 2p
\end{gathered}
$$

These nuclear fusion reactions basically power up the star and prevent the gravitational collapse of the star upon itself due to its mass.

Cosmic ray particles are accelerated by supernova shocks and have to travel through the interstellar medium before reaching us. The interstellar medium consists of various magnetic fields and radiation fields which these particles have to overcome. These fields cause the scattering of cosmic ray particles and therefore even if they reach us they have no memory of their sources.

Cosmic ray nuclei also react with particles in the interstellar medium to produce all kinds of secondary particles. It is known that 90% of the interstellar medium consists of hydrogen iodide and H_2 and 10% of it is made up of Helium and other heavy nuclei.

Finally when they reach our solar system they also have to overcome the magnetic field created by the Solar wind. The lower the 'rigidity' of the particle the lower is the

probability of it penetrating through the field. Rigidity refers to the charge to mass ratio of the particle. A lower ratio leads to particle being called more rigid and vice versa. Solar winds originate from the Solar corona and contain a variety of charged and neutral particles. They are carried along the magnetic field lines of the Sun. Solar winds are released from the hot coronal regions of the Sun. The number of Sunspots is a good reflection of the Sun's coronal activity at any given time. Increased number of sunspots means increased activity. The number of these sunspots on the Sun varies with a 11 year periodic cycle and also the Sun's magnetic field reverses its poles after every 22 years. Both these processes modulate the flux of the cosmic ray particles which eventually reach the Earth.

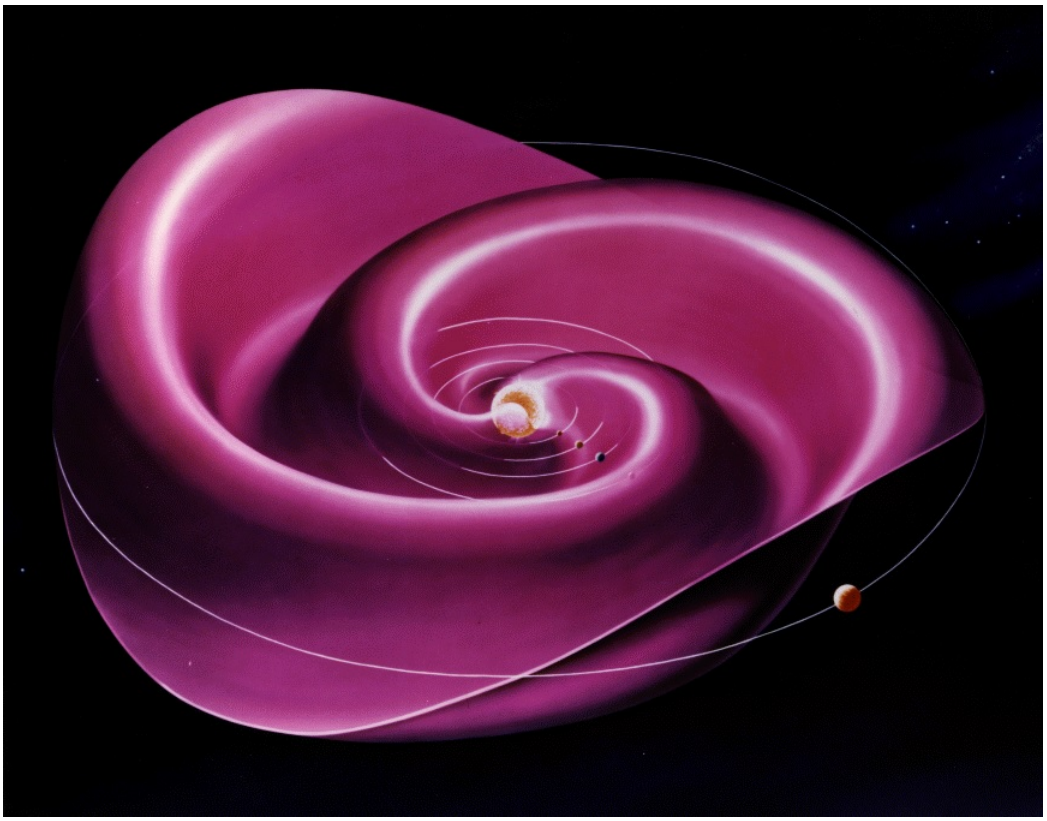

Figure 1.1: The heliospheric current sheet results from the influence of the Sun's rotating magnetic field on the plasma in the interplanetary medium (solar wind). The wavy spiral shape has been likened to a ballerina's skirt. [Courtesy-Wikipedia "Solar Wind"]

1.1.1 Cosmic rays at Earth

The atmosphere of Earth provides more than ten interaction lengths for protons going straight down. Interaction length is the mean free path length required to reduce the numbers of relativistic charged particles by the factor 1 exp as they pass through matter. And the energy loss of these cosmic ray particles fluctuates from event to event. Heavier nuclei have significantly shorter interaction lengths and lose energy much faster.

Comic ray particles interact with our atmosphere particles in three basic ways:

1. Electromagnetic interactions of charged particles; which are important for the prorogation of electron and photons through the cascade of reactions that occurs once the particles have entered our atmosphere.

2. Inelastic Hadronic interactions; that are important for the production of secondary particles such as pions which then further lead to the production of Muons.

3. Nuclear decay interactions; when heavier nuclei decay into lighter ones.

The last hurdle the particles have to face is the geomagnetic field of the Earth. The flux of the charged particles on Earth also depends on the latitude and longitude of the place from where they are being observed. This is due to variations in the strength of geomagnetic field with changing latitude and longitude. Magnetic fields always apply centripetal force on charged particles. There is general east-west effect in the flux of the charged particles. The direction of the geomagnetic field is such that more primary cosmic rays, i.e Hydrogen and Helium nuclei and atoms, come from west rather than the east.

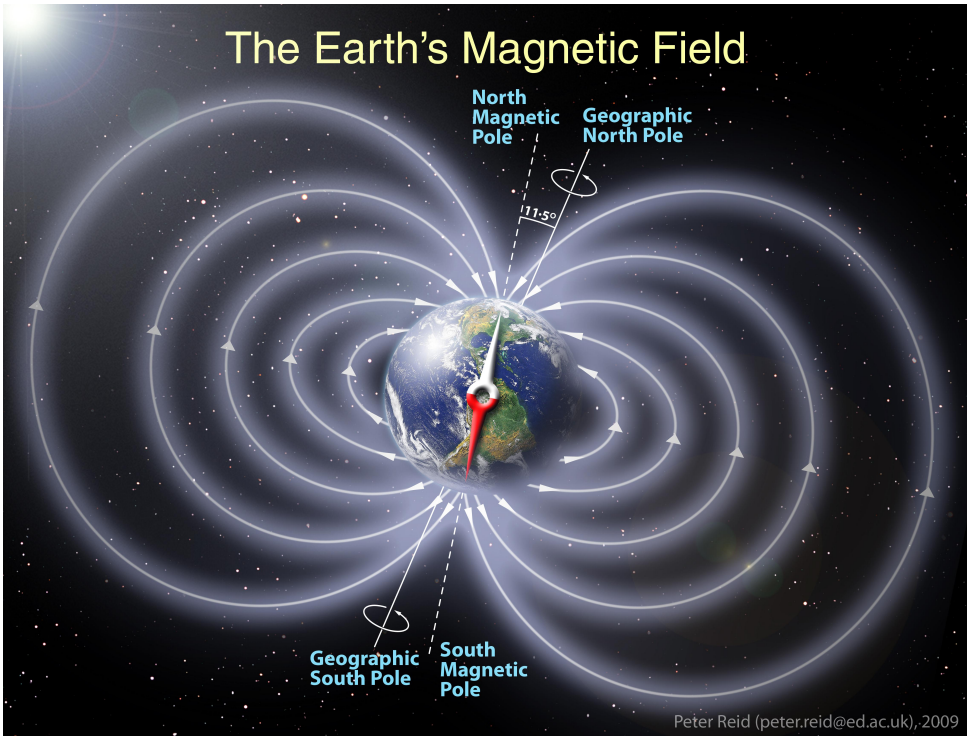

Figure 1.2: The Earth's magnetic and geographic poles. The white arrows show the direction of the geomagnetic field. [Courtesy-Wikipedia"Geomagnetic field"]

The particles coming from a general west direction are bent downwards towards the Earth's atmosphere while the ones coming from a general east direction are bent away from the Earth's surface. At higher latitudes the effect is stronger due to higher strength of the geomagnetic field and this effect is strongly noticeable.

Once these particles have entered our atmosphere and interacted with the air molecules they begin a cascade of nuclear reactions starting from the top of the atmosphere all the way to ground. At ground level these are known as cosmic ray showers. And they have two components to them: the 'soft' electromagnetic component and the 'hard' muonic component.

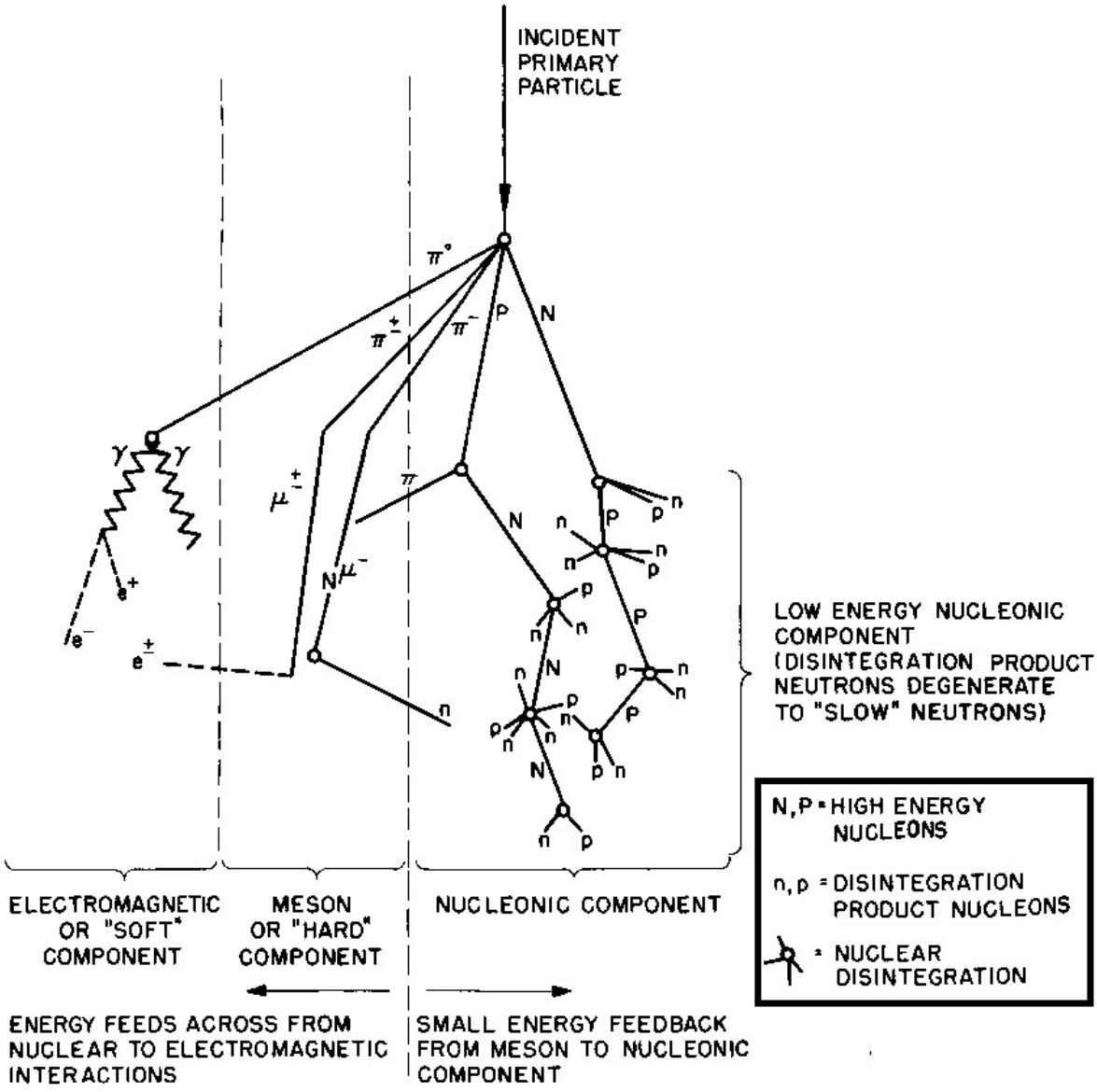

Figure 1.3: A general schematic representation of particle production in the atmosphere. It shows moderately energetic collisions taking place. Unstable particles like pions decay and electrons and photons undergo Bremsstrahlung and pair production, respectively [2].

Figure 1.3 shows a general schematic representation of these cosmic ray showers. By measuring the mass, charge and energy of a particle at a certain altitude we can determine what exactly the particle was and what is its place in the cascade. Measurements are usually performed by detectors placed on hot air balloons, airplanes or by satellites high up in the atmosphere.

1.2 Secondary Cosmic Rays: Muons

Muons are approximately created around 30 km up in the atmosphere [3]. Muons coming from the atmosphere have speeds very which are very close to the speed of light, c. Considering their velocity to be $0.98c$ for now for some back of the envelope calculations. At speed 0.98 c muons take roughly around $10^4 s$ from a height of 30 km to reach the ground. This is very intriguing as their lifetime is of the order $10^{-6} s$. When it was observed and noticed at first it was one of the first indications of time dilation, an effect predicted by General Relativity for particles travelling at speeds close to the speed of light. Time dilation basically says that the time experienced by muon in its rest frame 'slows' down as compared to the time in Earth's rest frame. Mathematically it is written as [4]:

$$t_\mu = \frac{t_{Earth}}{\gamma} \tag{1.1}$$

Here γ is the Lorentz factor which is written as $\gamma = \frac{1}{\sqrt{1-(\frac{v_\mu}{c})^2}}$. t_μ is the time taken in the rest frame of the muon and t_{Earth} is the time taken in the rest frame of earth.

In calculations of secondary cosmic ray particles we have limited knowledge of the primary cosmic rays that produces them. Measurements carried out on the secondary cosmic rays include particle to particle ratios, energy spectrums, flux at various altitudes and lifetimes. The main parameter which concerns us when performing such calculations is the amount of matter above any atmospheric layer through which these particles had to pass. This is atmospheric depth measured in g/cm^2. Temperature and density variations affect the interaction of cosmic ray particles and air molecules in the atmosphere.

Muons are basically a more massive copy of electron with mass 105.66 MeV and are spin-$\frac{1}{2}$ particles. The reactions which producing muons occur through weak interactions and are:

$$\pi^- \rightarrow \mu^- + \overline{\nu}_\mu$$
$$\pi^+ \rightarrow \mu^+ + \nu_\mu$$

Kaons also decay into muons by similar processes however muons produced by pions contribute to 95% of the incoming muon flux at ground level. After taking into account muons produced by both the processes the following equation can be derived which tells us about the energy spectrum of muons [1]:

$$\frac{dN_\mu}{dE_\mu} \simeq 0.14 E_\mu^{-2.7} \left(\frac{1}{1 + \frac{1.1 E_\mu \cos\theta}{\epsilon_\pi}} + \frac{0.054}{1 + \frac{1.1 E_\mu \cos\theta}{\epsilon_K}} \right) \tag{1.2}$$

Here the first term represents the contribution to the flux of muons by pions and the second term is due to contribution of kaons. Here $\epsilon_\pi = 115$ GeV and $\epsilon_K = 850$ GeV are the average kaon and pion energies as measured in the atmosphere. The weight of the kaon contribution 0.054 comes from the kaon production cross-section and contribution of kaons to the incident muon flux. This equation does not take into account the energy loss of the muons and therefore only gives good approximate results when high energy muons are considered.

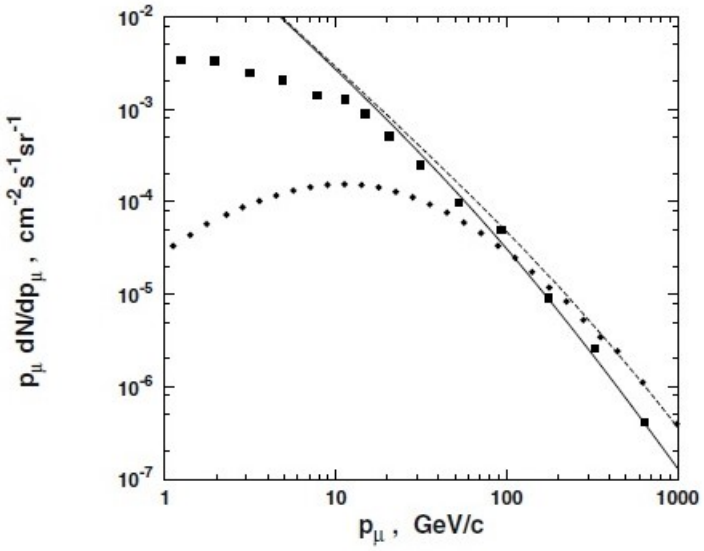

Figure 1.4: The muon flux spectrum given by equation 1.2 is shown by 1)the solid line which is for the vertical flux and 2) dashed line is of 75^o. [1]

Figure 1.4 is quite revealing in several ways. In the low energy limit where $E_\mu \ll \epsilon_\pi$ the spectrum is very similar to the energy flux spectrum of primary cosmic rays. However at high energies it steepens by one power of E_μ and the flux decreases sharply because at high energies the atmosphere does not provide enough space for the pions to decay and therefore Muon production decreases. The pion decay length at $E_\pi = 1000$GeV is 55.7 km in Earth's rest frame and this length is longer than the vertical extent of the atmosphere. And because of the $\cos\theta$ factor, which comes in equation 1.2, high energy pions decay more easily in nonvertical showers which leads to the Muons having a flatter energy spectrum at large angles. One more important thing to realise is that at low values of E_μ the contribution to the muon flux by the kaon factor also increases and can go up to 27% asymptotically.

At low muon energies the muon flux increases in general as the angle increases as shown by Figure 1.5. The exception to this general trend are the high energy muons , i.e. $p_\mu = 1000$ GeV/c, which are not affected that much and their flux steadily decreases with increasing angle. When the energy of a muon lies in the limit $E_\mu \geq \epsilon_\pi$ then the ratio of the inclined to vertical flux remains fairly constant even at large angles.

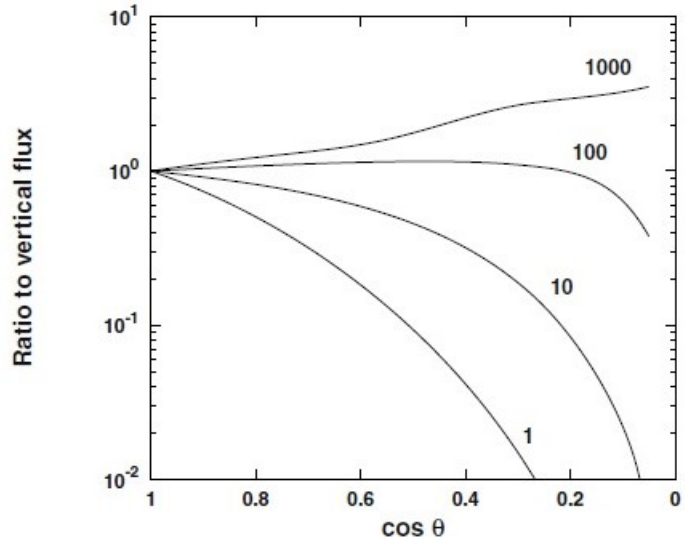

Figure 1.5: The ratio of inclined to vertical muon flux as a function of cos(θ). Each curve gives Muon momentum in GeV/c [1].

Figure 1.5 shows a Monte Carlo simulation which takes into account the curvature of the Earth. At energies lower than ϵ_π the ratio sharply decreases due to large amounts of energy losses mainly because of the increased amount of thickness of the atmosphere that the muon faces.

One last thing that will concern us is the muon charge ratio known as $R = \frac{F_{\mu^+}}{F_{\mu^-}}$. Here F_{μ^+} and F_{μ^-} are the respective muon fluxes of μ^+ and μ^- measured for varying momentum values of the muons. Due to the large flux of protons amongst the primary cosmic ray particles, R always has a value slightly greater than 1 as reactions of the kind $p + p \rightarrow n + p + \pi^+$, the number of π^+ are always more than the number of π^-. This also gives the overall particle cascade a net positive charge. As μ^+ are produced from π^+ and μ^- from π^- R is basically the π^+/π^- production ratio. In this experiment the value of R used will be $R = 56/44 = 1.27$ [4]. The relation of the ratio R and muon momentum can be seen in Figure 1.6 [1].

An atmospheric depth of 3.9 g/cm^2 corresponds to an altitude of about 40 km which is the decay length, l_d, of $\sim$ 7 GeV muons. Muons in the high energy range, 1 GeV, are produced further down in the atmosphere in between 30 to 20 km which is around one muon decay length to the observational level on the ground.

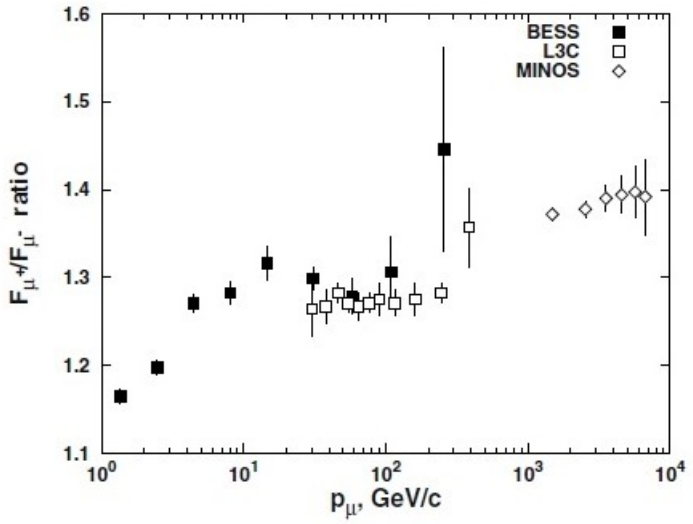

Figure 1.6: As the energy increases the Muon charge ratio also increases. This graph shows data from the experiments BESS, MINOS and L3C. The MINOS contributions that the higher value of ratio at higher energies is due a larger contribution by Kaons. At high energies K^+ are more commonly produced than K^- [1].

Chapter 2

Muon Lifetime Experiment

Muons decay through the following weak interaction processes:

$$\mu^- \rightarrow \nu_\mu + e^- + \overline{\nu}_e$$
$$\mu^+ \rightarrow \overline{\nu}_\mu + e^+ + \nu_e$$

We aimed to measure the time interval from the point where the muons entered our detectors to the point they decayed in the detectors releasing electrons. Our detectors were basically combination of Photomultiplier tubes and plastic scintillators whose workings are explained in Section 2.1. Electric pulses generated by these detectors were then refined and filtered using discriminators and electronic logic units. A Time-to-Analogue converter and an MCA were used to generate exponential distribution of the time interval on the computer. The distribution was fitted with an exponential function whose gradient gave us the mean lifetime of the muons. Figure 2.1 shows a circuit diagram of the whole experiment.

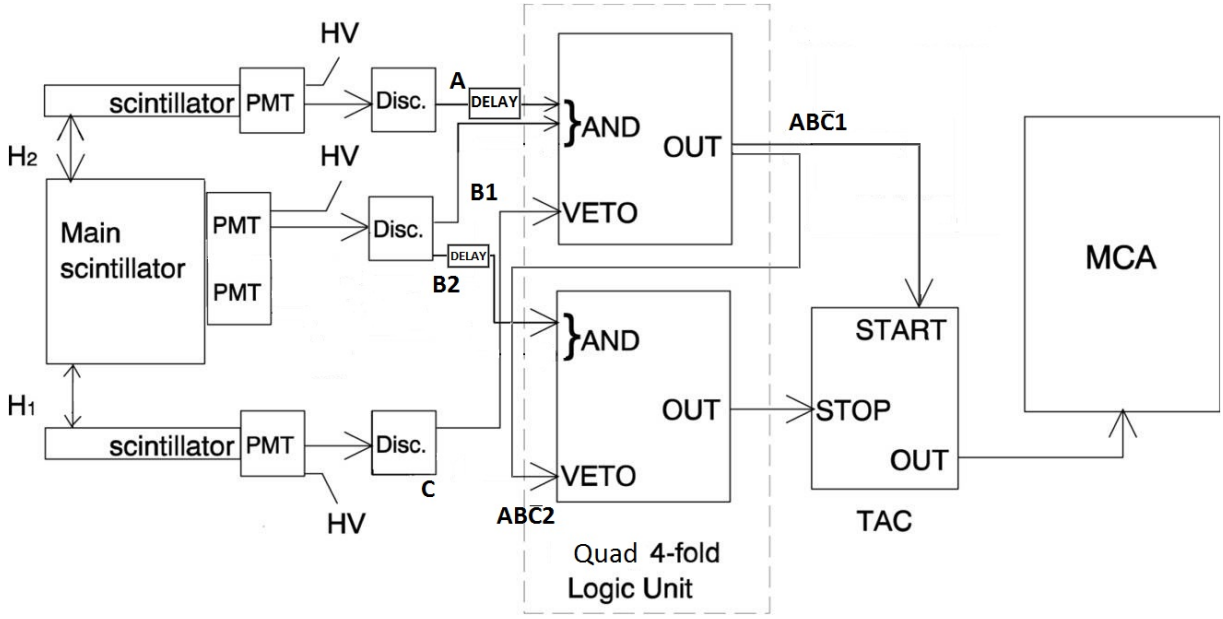

Figure 2.1: The circuit diagram of the Muon lifetime experiment.

2.1 PMTs and Scintillators

Scintillators: A scintillator is a material which fluoresces when a charged particle passes through it and excites its atoms. There are several types of scintillators which include both organic and inorganic scintillators. Plastic scintillators have a fairly high light output and a relatively quick signal with a decay time of around 2 to 4 ns. The biggest advantage with plastic scintillators is that they can be shaped into anything desired for the experiment.

Polyvinyl toluene, which is a plastic, scintillators were used in this experiment. Polyvinyl toluene has a refractive index of 1.58. Three plastic scintillators used for this experiment. Their shapes were in the form of paddles as shown by the Figure 2.2. Two of them had the same dimensions of $20 \times 300 \times 500$ mm ($h \times w \times l$) and the 3^{rd} one had dimensions of $100 \times 300 \times 500$ mm. The scintillators were wrapped in alluminized mylar sheets which are highly reflective and then were made light tight by covering them with black tape.

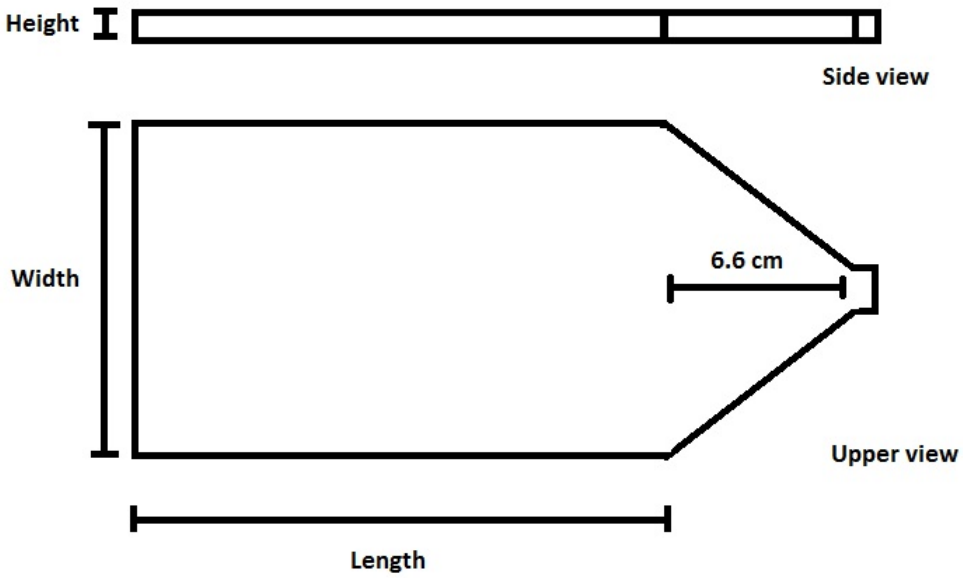

Figure 2.2: Plastic scintillator dimensions. Scintillators were made to custom and delivered by *REXON*. [5]

Photomultiplier tubes(PMTs): These tubes are vacuum tubes which are extremely sensitive detectors of light in the ultraviolet, visible and near infra red region of the electromagnetic spectrum. These detectors are able to amplify the current produced by light signal by a 100 million times. This is allowed by the several dynode stages present in the tube and this enables us to detect even single photons in the scintillator.

As can be seen in Figure 2.3 when a photon strikes the photocathode in the PMT it causes the cathode to emit electrons due to the photoelectric effect. The electrons released are then collimated using the focusing electrodes and are accellerated towards the dynode. Dynodes are electrodes assembled in a series inside the PMT with each successive electrode being more positive than its predecessor. On hitting the dynodes

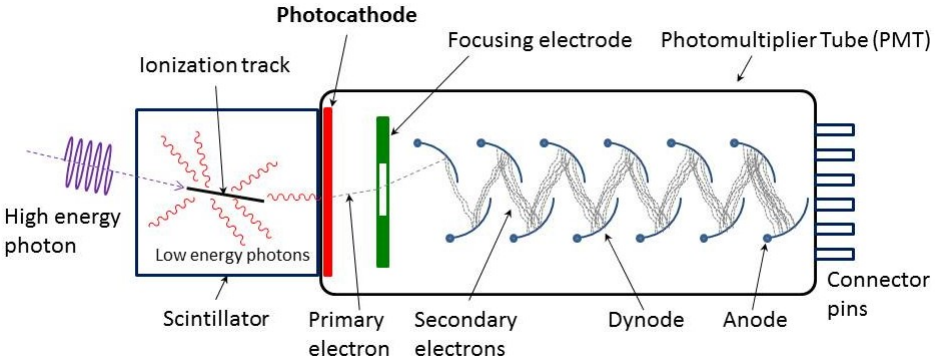

Figure 2.3: Workings and the internal structure of a PMT. [Courtesy, Wikipedia- "Photomulitplier tubes"]

electrons cause secondary electron emissions. Therefore at each dynode stage more and more electrons are released amplifying the signal. These electrons then finally reach the anode which gives us the output in the form a electric pulse.

Three PMTs were used in our experiment; one for each scintillator paddles. Two identical smaller ones (20 mm diameter PMT) for the thinner paddle and the bigger one (80 mm diameter PMT) for the thicker paddle[1].

The PMTs and scintillators joined together were collectively referred to as a detectors. The three of them were labelled as A, B and C respectively with detectors A and C being the identical smaller ones with 20 mm diameter PMT. And the detector B would be the larger and thicker paddle joined with the 80 mm diameter PMT.

Figure 2.4: Detector B covered in black tape. Consists of 100 mm height scintillator covered in alluminized mylar sheet and the 80 mm diameter PMT.

[1]The PMTs used with their respective model numbers were Hamamatsu E990MOD2 for the 20 mm and REXON $RB14-8E$ for the 80 mm one.

2.2 The Experimental setup

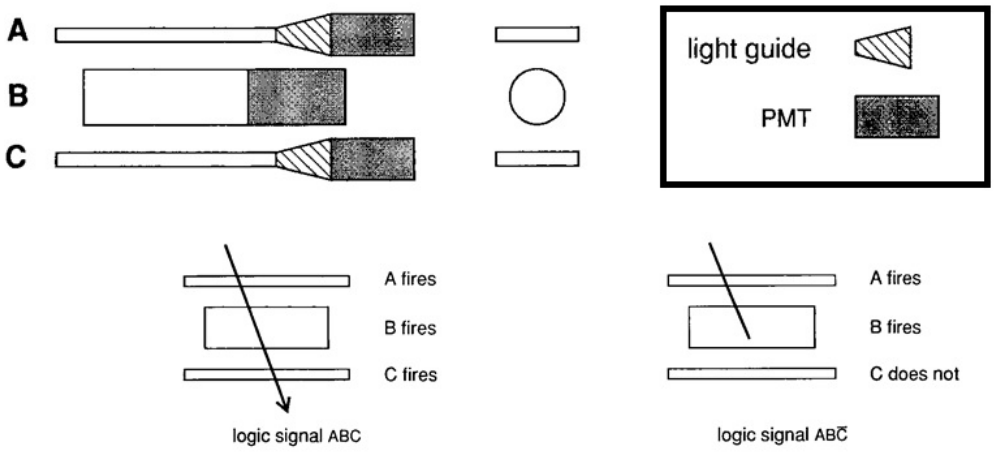

Figure 10a Muon penetrates A and B and C. **Figure 10b** Muon stops in B and then decays.

Figure 2.5: The three detectors are placed such that B is sandwiched between A and C for the experiment. When a Muon passes through all three detectors, all three generate pulses. This is known as an ABC signal. When the Muon is stopped in B, only A and B detector generate pulses. These together are known as the AB$\bar{\text{C}}$ signal. [3]

The plastic paddles of detectors A and C were relatively thin and therefore generally were unable to stop the incoming muons. However there was a very large probability that paddle B, which was five times thicker than A and C, would stop the incoming muon inside it.

There were slabs of foam placed between the three detectors therefore each of them was about 20 mm away from each other. As Figure 2.5 shows when a muon passed through all three detectors and escaped all three would generate a pulse. These pulses together were known as the ABC signal. If the muon stopped in B then we had the signal AB$\bar{\text{C}}$.

In this experiment the lifetime of the muon in its rest frame was measured. When the muon was stopped in detector B the pulse generated was the AB$\bar{\text{C}}$. And then when the muon decayed in B a second pulse was generated by B as the muon released an electron or a positron depending on whether it was μ^- or μ^+. Measuring the time difference between the AB$\bar{\text{C}}$ and B pulse gave us an exponential time distribution the gradient of which was the mean lifetime of the muon.

The mean lifetime of the muon in its rest frame is known to be $(2.197 \pm 0.00004)\mu$s. In free space both the muons, μ^- and μ^+, have the same lifetime. However in the plastic scintillator the lifetime of μ^- decreased to around 1.7×10^{-6} s [4]. μ_- decay faster because they decay by two processes in the plastic scintillator, muon capture and muon decay. Muon capture refers to muons being absorbed by nuclei of atoms of Polyvinyl toluene. Furthermore $\mu-$ are vulnerable to capture by positive high-Z nuclei (i.e. carbon Z=6) of atoms and the effect is noticeable.

2.3 Electronic units

2.3.1 Logic untis

An electronic unit was needed such that if pulses arrive from A and B together in time then only an output pulse would be generated called AB$\bar{C}$. And only AB$\bar{C}$ and the second B pulse were allowed to go ahead. However if pulse from C also arrived with A and B pulses then the signal was rejected. For this, electronic logic units were required. ABC signal pulses were rejected because ABC pulse would basically indicate that the muon passed through all three of our detectors and escaped and therefore the signal would be of no use to us. For similar reasons other pulses also needed to be rejected.

We used Phillip Scientific's Quad Four Fold Logic Unit Module (Model 755). The four fold module has basically four logic units in it. The design and the workings of the logic unit 1 are explained using Figure 2.6. All logic units work in the same way but are used differently. Logic unit 1 will be used to generate AB$\bar{C}$ pulse.

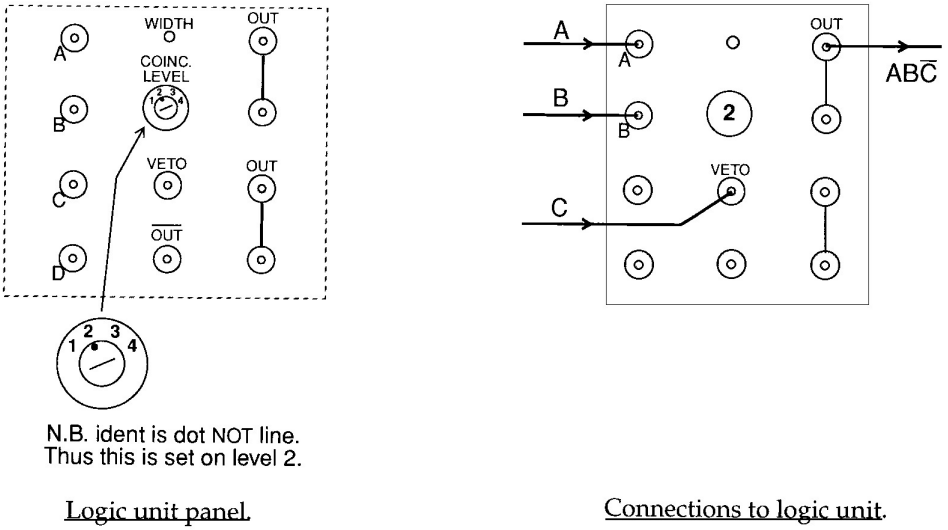

Figure 2.6: Logic unit 1 of the Quad Four Fold [3].

If logic unit 1 got a pulse from A and B simultaneously then it generated an output pulse. This was ensured by keeping the logic unit at coincidence level 2 so that it acted as AND gate for A and B pulses. However if it also got a pulse from C detector, the output pulse of the logic unit was then 'vetoed' or cancelled.

2.3.2 Discriminators

However one really important thing we are missing here that logic units only work with negative square pulses which are also known as logic pulses. Pulses from the PMT's are negative but not square in shape.

Figure 2.7 and Figure 2.8 show pulse waveforms from PMTs B and C respectively as seen on our oscilloscope. They are not certainly square in shape. To make them into

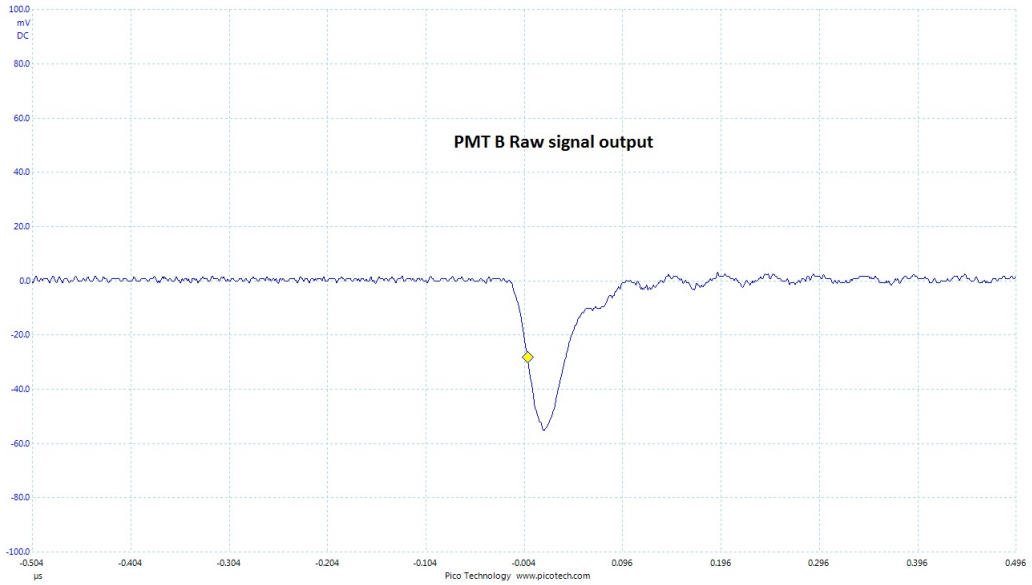

Figure 2.7: Pulse from PMT B

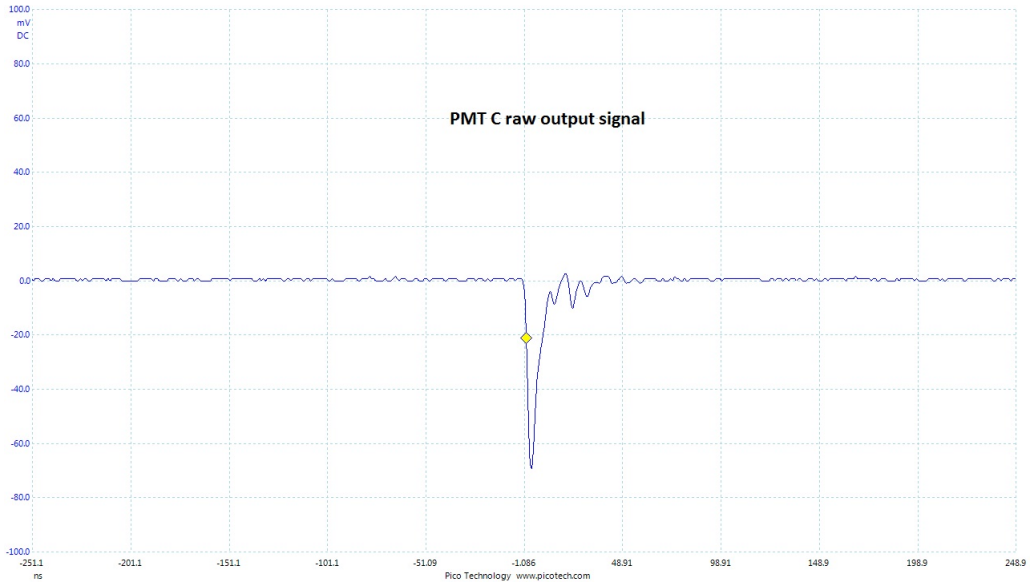

Figure 2.8: Pulse from PMT C. Pulse from PMT A would also be very similar to pulse from C as both PMTs are indentical.

logic pulses we need to first pass them through another type of electronic unit known as the discriminator.

Discriminators take PMT pulses and produce negative logic pulses if the PMT pulses exceed a certain threshold voltage. That threshold can be adjusted during the experiment. And it helps to eliminate the electronic noise which is present at very low voltage. This makes sure that a logic pulse would only be generated if the detector has actually 'seen' a particle and would not be generated by some small random electronic fluctuation.

In our case we used Phillips Scientific's Octal Discriminator Unit Module (Model 705). It basically has 8 discriminators in it. Each discriminator unit has the channels as shown in Figure 2.9.

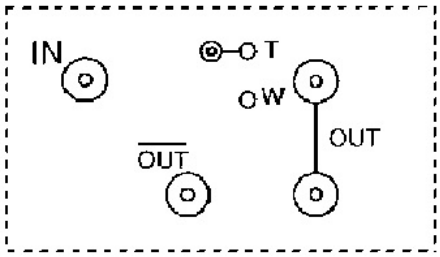

Figure 2.9: A single discriminator unit interface [3].

The threshold was varied by adjusting the potentiometer using a trim tool. Width of the pulse was controlled by using the trim tool in the W channel. The discriminator had two negative output outlets and one inverted (i.e positive). output outlet.

2.3.3 Time-to-Amplitude Converter (TAC) and the delay box

Each PMT pulse was first passed through the respective discriminator unit. The pulses from the discriminators were then passed onto into logic unit 1. However no method had yet been figured out to measure the time difference between the AB$\bar{C}$ and B pulses. It was realised that this could be done by using a TAC.

A TAC measures the time interval between two pulses and then generates an output pulse of magnitude proportional to the time interval. The time to voltage scale of the TAC can be varied. For the muon lifetime experiment the scale was kept at 10μs. This meant that time difference of 2μs would generate a positive square pulse of amplitude 2 V. If the time difference exceeded the time scale then that pulse was rejected and the TAC was reset. The TAC has two inputs the START and the STOP and one output called OUTPUT. The whole experimental setup is shown in Figure 2.1.

In our experiment we used the Ortec TAC/SCA Model 567. The AB$\bar{C}$ was fed into the START input of the TAC. A second output, B2, is taken from the discriminator unit of PMT B and was fed into the STOP input of TAC.

However this was not correct. It is because the detector B generated two pulses when a muon stopped in it. Although the AB$\bar{C}$ pulse started the TAC but the first B pulse stopped the TAC as soon as it started. Therefore to avoid this first pulse stopping the TAC, a second output from the B discriminator unit, called B2, was first connected to the input channel of logic unit 2. And a second output of the AB$\bar{C}$ called AB$\bar{C}$2 pulse was connected to the VETO input of logic unit 2. Logic unit 2 was kept at coincidence level 1 and is shown in Figure 2.10.

When the B2 pulse and the AB$\bar{C}$2 pulse were in sync the first pulse from detector B got vetoed and rejected and only the second pulse from B was allowed to go forward to the STOP input of TAC.

At this point we finally come to the point where all the delays which are required to make this setup work were introduced. As we discussed earlier PMT B was bigger than both PMTs A and C. Therefore it also took more time to give out a pulse as

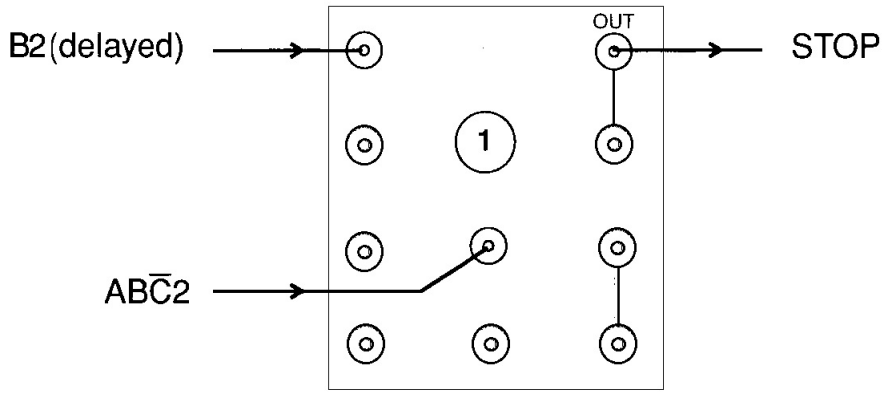

Figure 2.10: The connections made on logic unit 2 [3].

compared to the smaller PMTs. For logic unit 1 to work we needed to have the A and B1 pulses coming at the same time. Therefore we had to delay the A pulse such that it coincided with the B1 pulse. This delay in our case was round about 33. ns and was empirically selected. This was done by introducing a electronically passive delay box. It was a Stanford Research Systems delay box Model DB64. The PMT A pulse was then first passed onto delay box and then from the delay box it went to the discriminator unit. The width of B discriminator pulse was also increased because PMT B generated a large amount of jitter in its pulse due to relatively more dynode stages than A and C and also because it operated on higher voltage. The A and B discriminator pulses are shown in Figure 2.11

PMT C pulse also had to be delayed to coincide with A and B pulses so that it can veto them if the muon passed through all the three detectors. The pulse was delayed by introducing a delay barrel before the pulse went to the discriminator unit. A delay barrel is an BNC connecter introduced between the wires. The A and C pulses are shown by Figure 2.12

One other delay which had to be introduced as shown in Figure 2.10 is that of the B2 pulse. The pulse had to be delayed such that it coincided with ABC̄2 pulse because the first B pulse has to be vetoed. B2 was delayed by introducing some extra limo cables. This causes B2 to coincide with ABC̄2. The output of logic unit 2 was then connected to the STOP input channel of the TAC. The ABC̄2 and B2 pulses in coincidence are shown in Figure 2.13

The output pulse generated by TAC which was a positive square pulse is shown in the Figure 2.14. A high speed digital oscilloscope was used to capture these pulse images.

2.3.4 The Multi-Channel Analyser (MCA)

The MCA is basically a device which takes only positive square pulses and distinguishes and counts them according to their amplitude (voltage). It contains channels and each channel corresponds to a specific voltage. Whenever the MCA receives a pulse of that amplitude it makes a count of on that channel. So each channel tells us that how many pulses the MCA received of that particular amplitude.

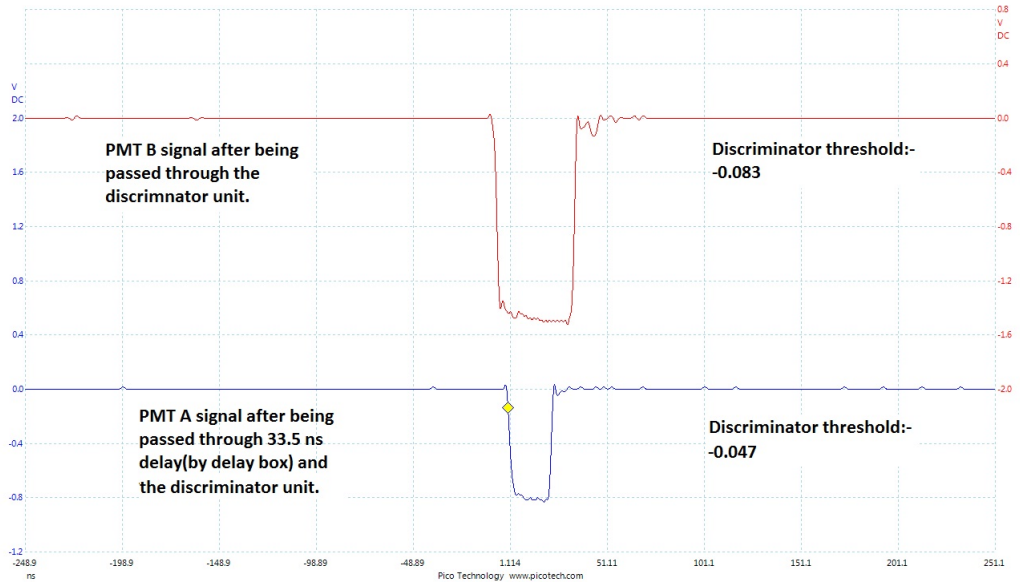

Figure 2.11: Pulses from A and B discriminator units in coincidence. A has been delayed by 33.5 ns to coincide with B. The width of B pulse is increased such that B coincides with A even if it jitters.

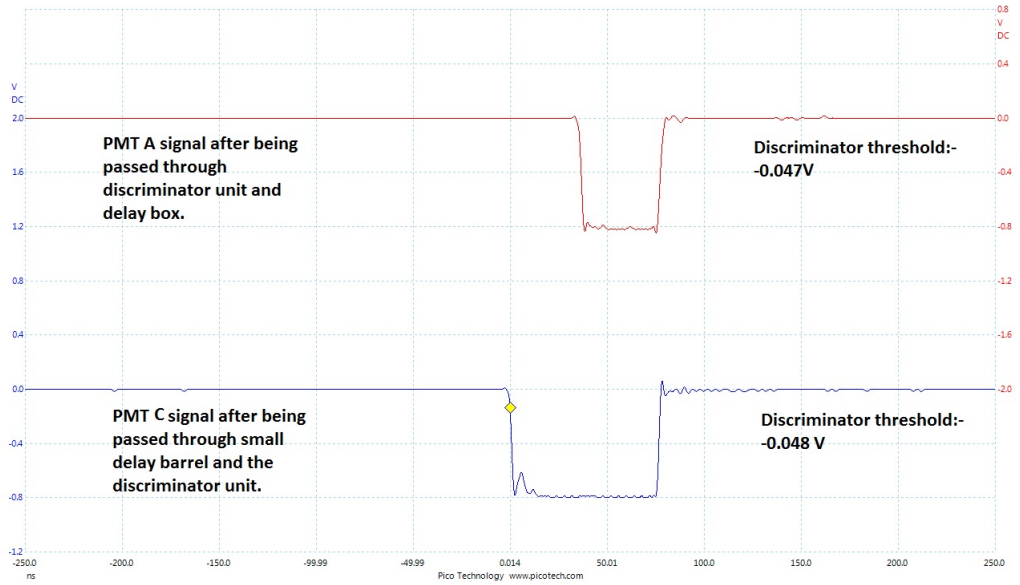

Figure 2.12: Pulses from A and C discriminator units in coincidence. C has been delayed by a delay barrel to coincide with A and B.

For our experiment we used AMPTEK's MCA8000D. This MCA accepts voltage pulses in the range 0-10 V which corresponds to the output voltage of the TAC which also generates pulses in this voltage range. Also this MCA has 8192 channels which means that it has a resolution of 10 V/8192 channels= 0.00122 V/channel. Using the data from the MCA a Count vs Channel histogram is generated. The histogram shows the number counts that each channel received for its specific voltage pulse. Channel scale is then first converted to voltage scale using the 0.00122 V/channel scaling factor of the MCA. The voltage scale is then converted to time scale using the V/s scaling factor of the TAC which in this case is 1 V/s. The histogram is then fitted with curve and using that the muon lifetime is calculated. This will be discussed in detail in the next section.

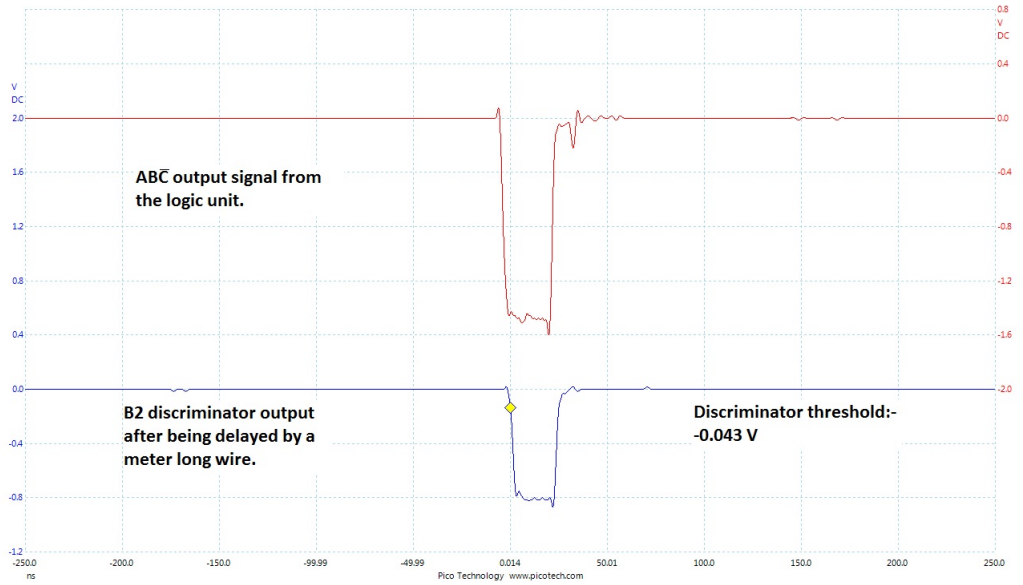

Figure 2.13: ABC̄2 and B2 pulses in coincidence. B2 has been delayed by adding extra limo cables in its path.

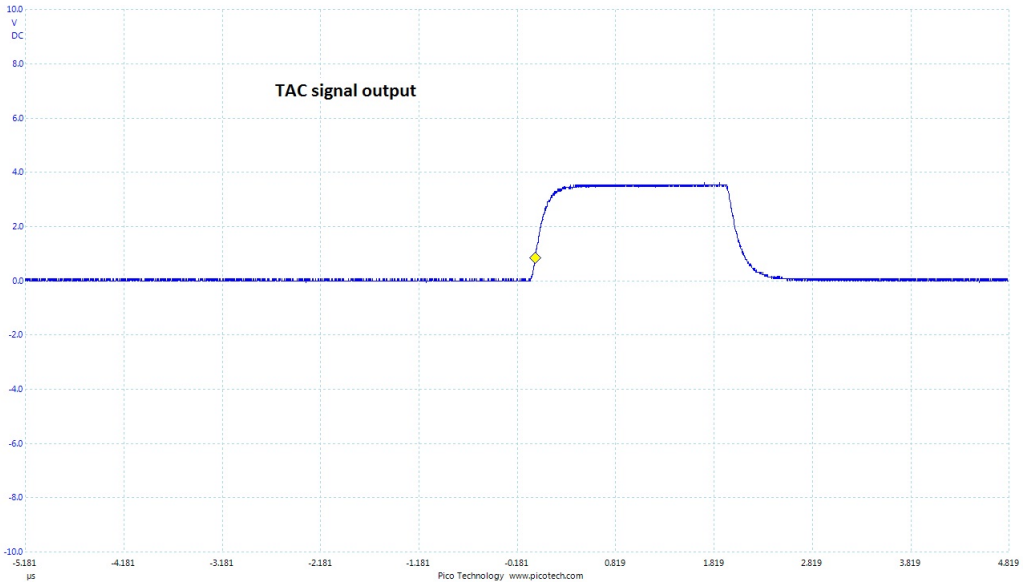

Figure 2.14: The TAC output signal.

Therefore the overall final circuit diagram of the whole experiment is shown in Figure 2.1. All of the workings discussed in this section are shown by this diagram.

Chapter 3

Optimisation and Analysis of the lifetime experiment

3.1 Optimising the experimental parameters

This experiment has six variables which have to be set before starting any experiment run. The six variables are:

1. PMT A voltage
2. PMT B voltage
3. PMT C voltage
4. Threshold of the A discriminator unit.
5. Threshold of the B discriminator unit.
6. Threshold of the C discriminator unit.

The next aim was to set the 6 experimental parameters to measure the mean muon lifetime.

3.1.1 Discriminator Thresholds and Voltages for PMTs A and C

An important thing to be realised was that the number of muons passing through the three detectors in a time interval was finite. Using this fact it could also be implied that if the voltages of A and C PMTs were increased then the number of muons detected in a fixed time interval should flatten off after a certain point. The spectrum shown in Figure 3.1 therefore was predicted.

We needed to find a relation between the muon flux between the detectors A and C and the voltages of their PMTs at a constant threshold. This was needed in order to predict the value of voltage (at a fixed threshold) above which the voltage did not

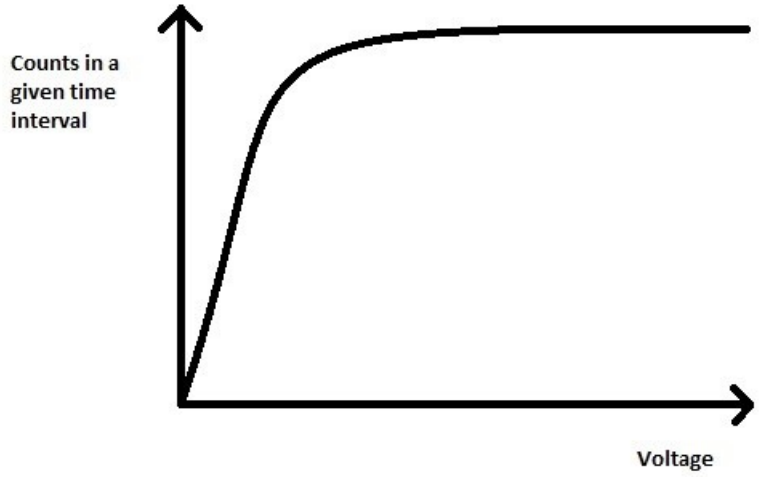

Figure 3.1: Expected spectrum (Count vs Voltage) of the number of counts through detectors A and C in a finite time interval.

affect the counts of the muons being detected in a time interval. To execute this idea experimentally pulses from detectors A and C were put in coincidence using a logic unit which acted as AND gate. Three main sets of data were taken for three thresholds of A and C discriminator units which were -30 mV, -40 mV and -50 mV. During any run these thresholds were identical on both A and C discriminator units. For each set the threshold was kept constant and the values of voltages of A and C together were varied from 850 V to 1250 V at an increment 50 V. The time interval for each experimental run in this case was 180 s.

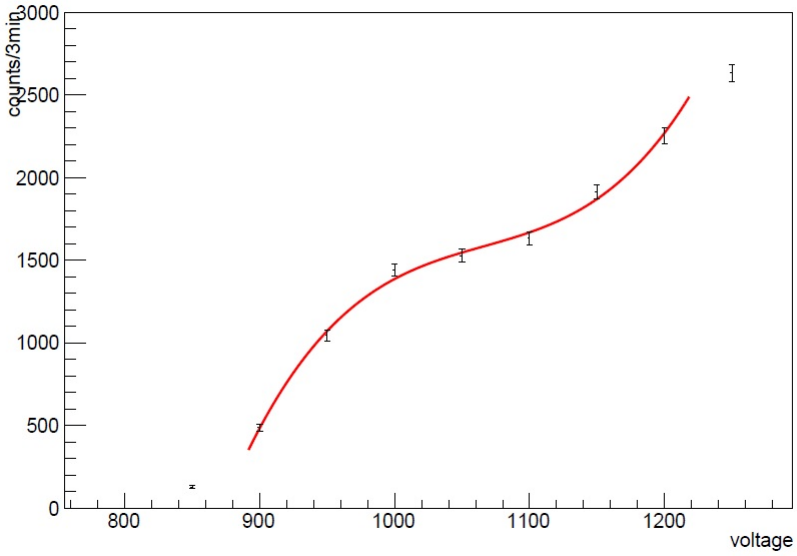

Figure 3.2: AC pulse counts against Voltage for -30 mV threshold.

Figures 3.2, 3.3 and 3.4 show the counts recorded for each of the voltages in the voltage range at a constant threshold value. A third degree polynomial was used to

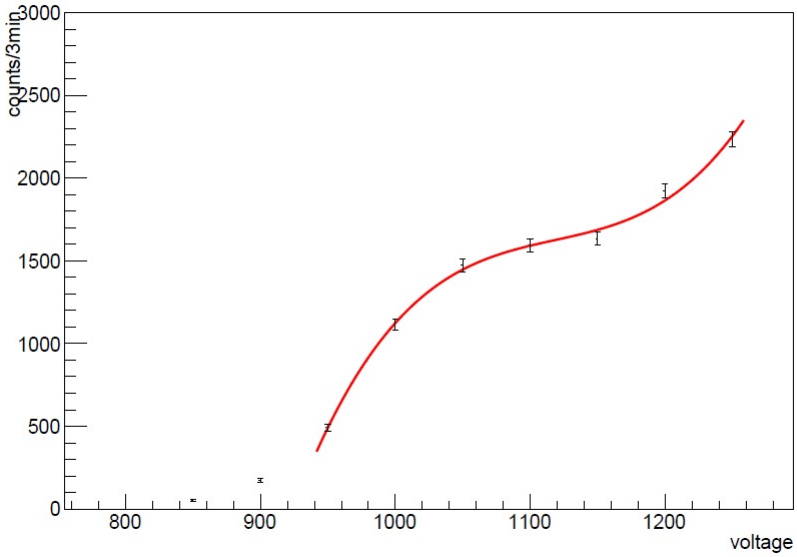

Figure 3.3: AC pulse counts against Voltage for −40 mV threshold.

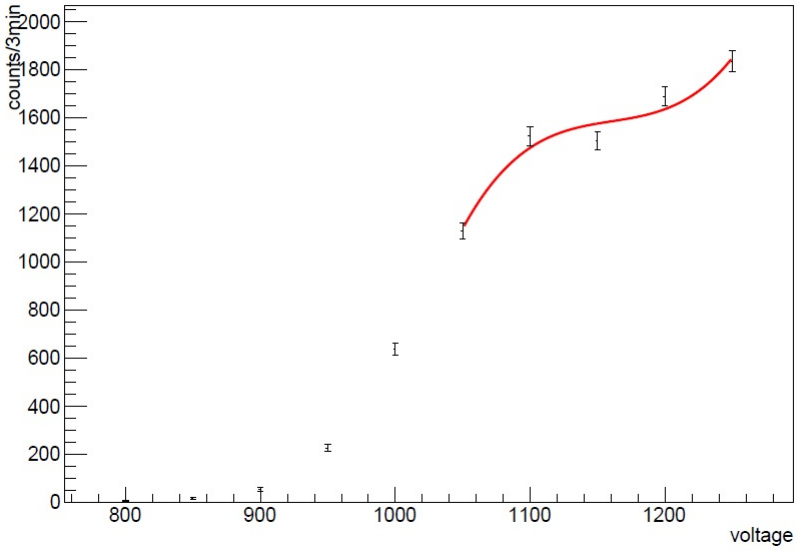

Figure 3.4: AC pulse counts against Voltage for −50 mV threshold.

fit all the curves. It can be clearly seen that all three curves flatten off at a certain point but then the number counts start to rise again. This is because above that voltage the noise also starts to get amplified. The respective voltage values at which the curve flattens off for each of the three thresholds are 1050 V for −30 mV, 1100 V for −40 mV and 1150 V for −50 mV.

After these results it was finally decided that each of PMTs A and C will now be run on 1100 V and the threshold of each of their discriminator units will be −40 mV. Therefore four of the six experimental variables were fixed at this point.

3.1.2 Efficiency of Detector B

For the last two parameters we decided to measure the efficiency of B at varying values of the voltage of PMT B and the threshold of unit B. Values of A and C PMT voltages and discriminator were fixed as discussed in the previous section. It was realised that by measuring the efficiency at different values we can pick only those values of voltage and threshold for which detector B was most efficient. And those will then be used in measuring the mean muon lifetime.

Efficiency is the probability of a particle being detected by the detector when the particle is passing through it. To measure the efficiency of a detector, ε, we place the detector, B, between two other detectors, A and C, whose efficiencies are ε_1 and ε_2 respectively.

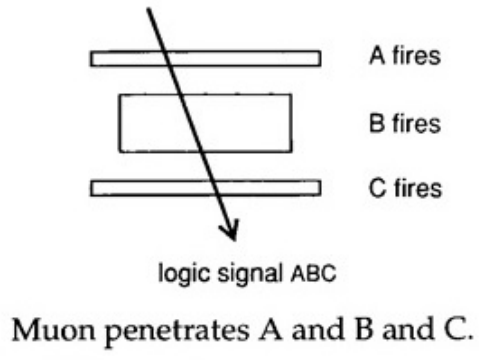

Figure 3.5: Threefold coincidence of the A, B and C detectors generating ABC signal pulse when a muon passes through all 3 of them [3].

A threefold coincidence is setup between the three detectors such that whenever a muon passes through them an ABC pulse is generated. All this process is done by using discriminators and logic units. A new logic unit is used where all three of the pulses from the A, B and C discriminators are put in coincidence after introducing specific delays as discussed in the previous section.

If the total number of muons that pass through all three detectors is N in a specific period of time, then the total number of ABC pulses, or N_3, generated in that time would be given by:

$$N_3 = \varepsilon_1 \varepsilon_2 \varepsilon N \tag{3.1}$$

Another twofold coincidence is setup between the A and C detectors at the same time. And the pulses generated by this coincidence are called the AC pulses. The total number of AC pulses or N_2 recorded in that time interval would then be given by:

$$N_2 = \varepsilon_1 \varepsilon_2 N \tag{3.2}$$

Dividing Equation 3.1 by Equation 3.2 would then give us the efficiency of detector

B:

$$\varepsilon = \frac{N_3}{N_2} \tag{3.3}$$

Therefore if somehow N_3 and N_2 could be measured for a particular set of values of the 6 parameters and for a particular time interval then the efficiency alone of detector B could be measured.

There were certain experimental challenges which had to be overcome for carrying out this process. The MCA we had only had one input and all MCAs accept only positive square pulses. As implied by the process in the previous paragraph the only things that were of concern to us were the number of pulses N_3 and N_2. An electronic circuit had to be developed which would allow the MCA to count AC and ABC pulses simultaneously on a single input.

This could be done if the pulses of AC and ABC had separate fixed amplitudes so that the MCA can distinguish between them. Separating the pulses on the basis of their amplitudes would allow us to feed these pulses to the MCA on single input. This is what the circuit shown in Figure 3.6 did. Outputs from the two logic units were first inverted to make them positive square pulses using the TTL (Transistor Transistor Logic) output available on the Phillips Scientific's Quad Gate/Delay Generator (Model 794). Then they were fed into the circuit shown in Figure 3.6. One of them, N_2, was delayed by 2.2μs using the delay generator so that ABC and AC pulses do not get mixed up. Separate resistances, 300Ω and 50Ω, to each of the two inputs gave them separate fixed amplitudes. Diodes were placed to further ensure that an AB pulse does not get mixed up with an ABC pulse or vice versa. The diodes used were 1N4148 diodes which are high speed diodes with a fast clocking time. The two inputs were then combined and input into the MCA using a single input.

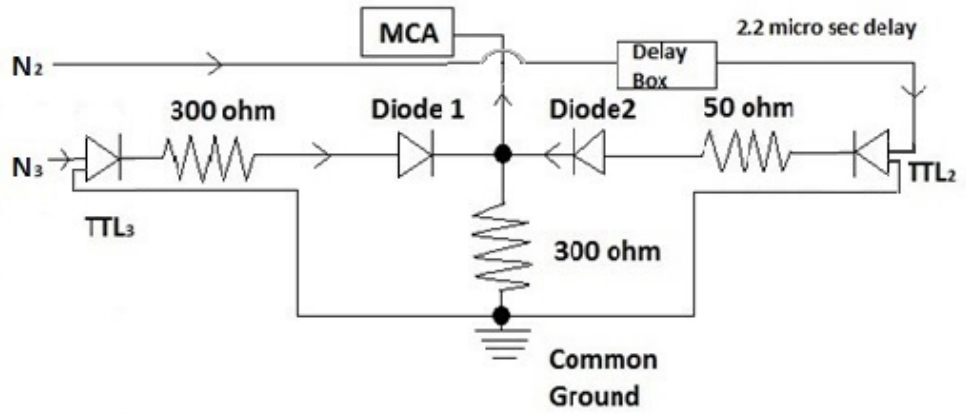

Figure 3.6: The circuit developed to allow the MCA to record the number of AC and ABC pulses at the sametime.

The result of this was two separate peaks of pulses on two separate channel ranges on the MCA spectrum as shown in Figure 3.8. The output of the circuit on the oscilloscope is also shown in Figure 3.7. The number of pulses N_3 and N_2 were then determined by counting the number of counts separately in these two peaks. Dividing

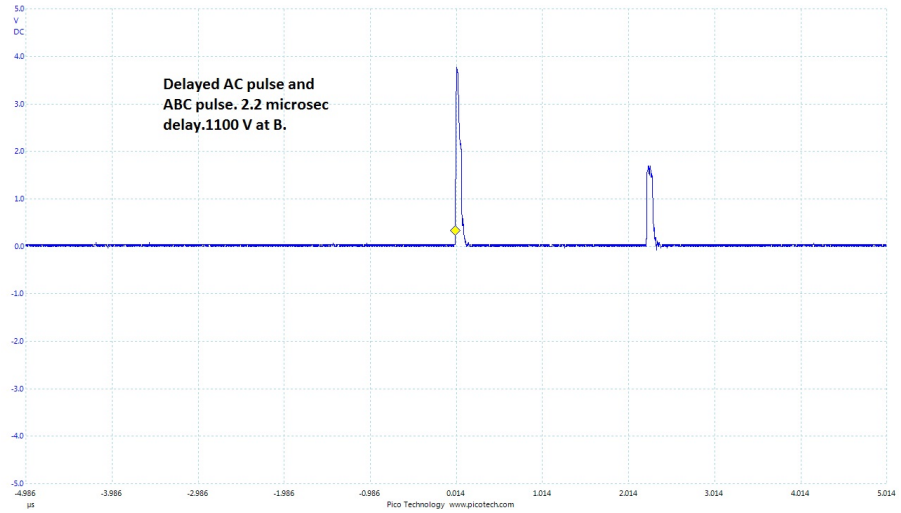

Figure 3.7: The output of the circuit shown in Figure 3.6 on the oscilloscope.

these two numbers then gave us the efficiency of B for that particular experimental configuration.

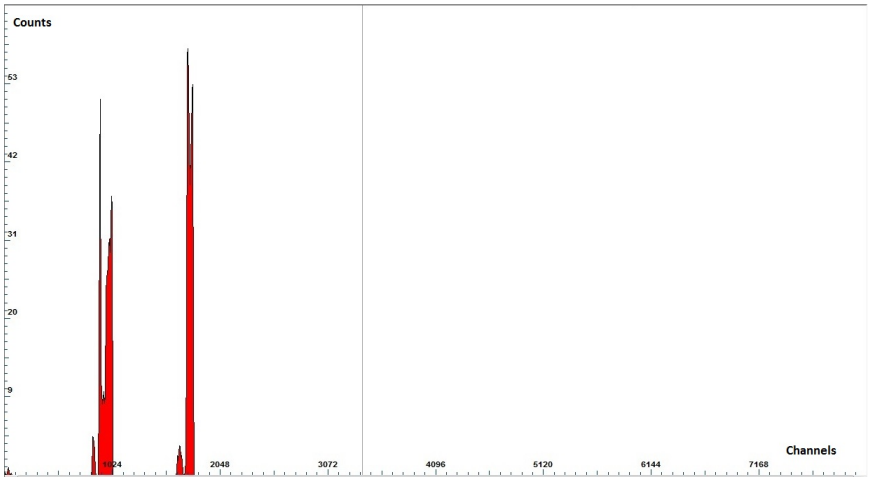

Figure 3.8: The output of the circuit shown in Figure 3.6 on the MCA spectrum.

The efficiency of B was calculated several times. The efficiency was very high and on average was equal to 99.6%. The delay between ABC and AC pulses was kept fixed at 2.2 μs. The threshold and voltage settings were same as that of initial muon lifetime runs.

These results very clearly indicated that at settings which were being used for the initial muon lifetime runs the detector B was highly efficient in detecting a particle passing through it.

3.1.3 Discriminator Threshold for PMT B

After determining the efficiency of B the next step was to fix the values of the voltage of PMT B and the threshold of discriminator unit B. And the first task was to set the discriminator threshold for B.

PMT B was larger than PMT A and PMT C and was operated at a higher voltage than A or C. Therefore it also generated more electronic noise. The voltage and the discriminator threshold of the detector B had to be set in such a way that the noise was minimised and the signal got sufficiently amplified. To do this the spectrum of detector B was observed at different voltages on the MCA software. The thresholds for A and C discriminator units were kept at -48 mV and for B at -83 mV for all runs.

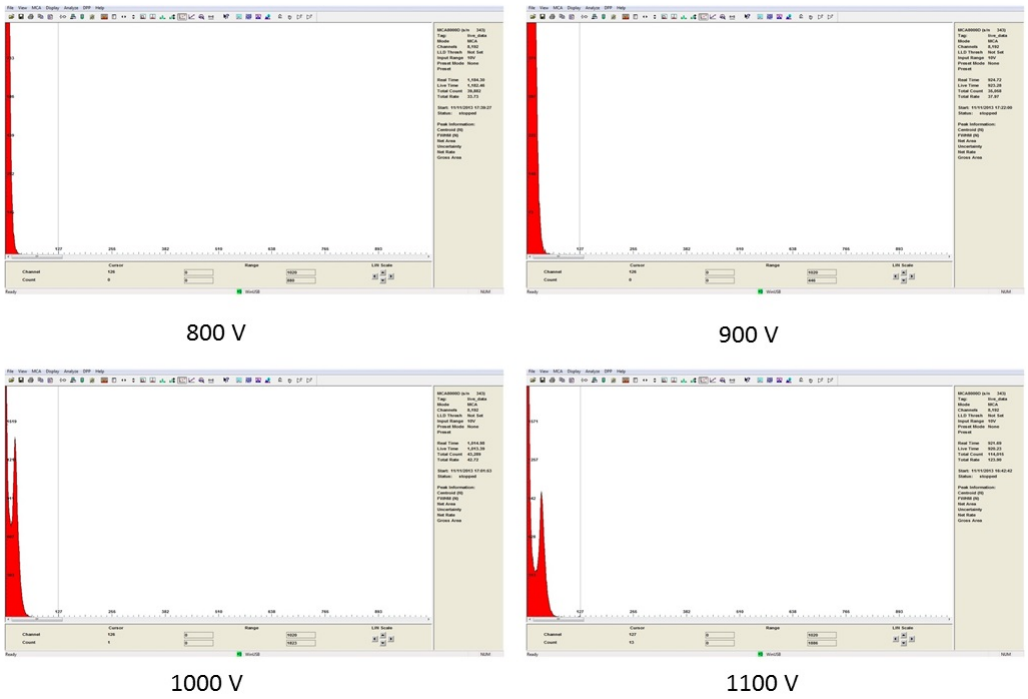

Figure 3.9: Spectrum of detector B at different voltages

Figure 3.9 shows the spectrum of B observed on the MCA at 800 V, 900 V, 1000 V and 1100 V. At low voltage a large noise signal can be observed. However as the voltage is increased we can clearly see a distinct signal peak which comes out of the large noise peak. This is believed to the background radiation signal. Two points around this peak were selected where the peak basically started and ended on the spectrum These two points roughly corresponded to 40 mV and 75 mV. Therefore it was decided that threshold for B would be kept at either of these two values of voltages. And then the efficiency of B would be measured again. However before doing that it was required that other parameters are also known. This takes us to the next section.

3.1.4 Voltage for PMT B

The only two parameters left at this point to be fixed were the voltage of PMT B and the threshold of the B discriminator unit also had to be decided between -40 mV and -75 mV. It was decided that the efficiency of B will now be calculated again. Two sets of readings would be taken at two separate fixed thresholds of B: -40 mV and -75 mV. The voltages for each of the two sets of data ranged from 600 V to 1300 V

with an increment of 50 V. The voltages and discriminator thresholds of PMTs A and C were kept at 1100 V and −40 mV as discussed in the previous section.

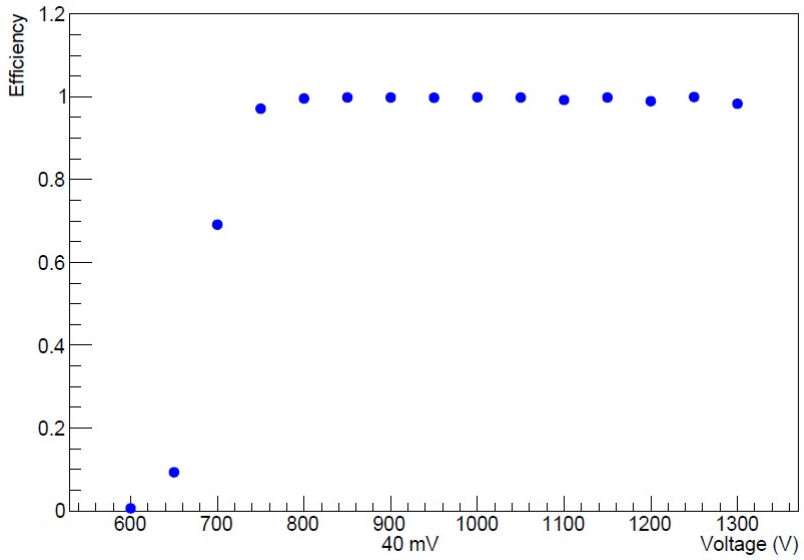

Figure 3.10: AC pulse counts against Voltage for −40 mV threshold.

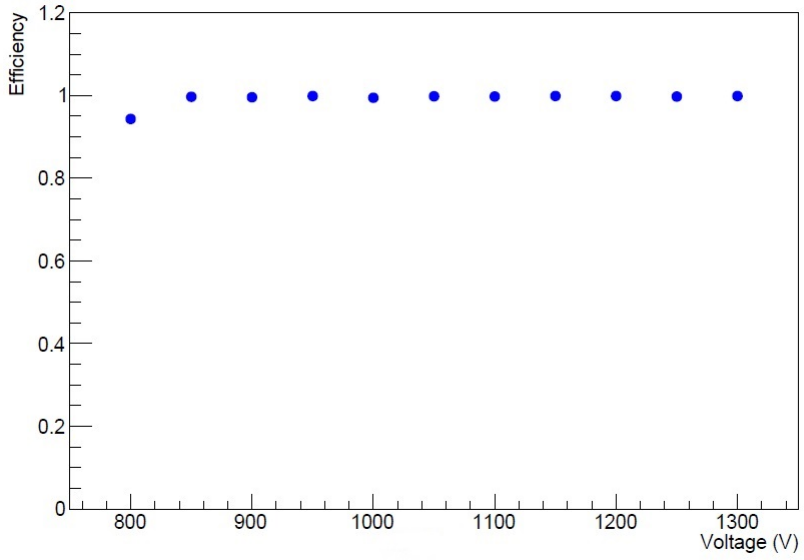

Figure 3.11: AC pulse counts against Voltage for −75 mV threshold.

As it can be seen the efficiency of B largely remained unaffected and consistently had a very high value for a large range of voltages. This can be explained by it being relatively more thick and having a PMT of larger diameter than A or C. This means that any muon had to travel a larger path detector B as compared to A or C and therefore more light was generated in B.

As PMT B generally tended to generate more noise and is larger therefore it was decided to operate it at a discriminator threshold of −75 mV and at a voltage of 1100 V.

3.2 Result and Analysis of the Final muon lifetime run

Now all the six experimental parameters had been fixed and their respective values were:

A,C voltage	1100 V
B voltage	1100 V
A,C threshold	−40 mV
B threshold	−75 mV

The muon lifetime experiment was run again several times. The lifetime experiments were generally run for around 30, 000 s. A typical result for muon lifetime is shown in the Figure 3.12.

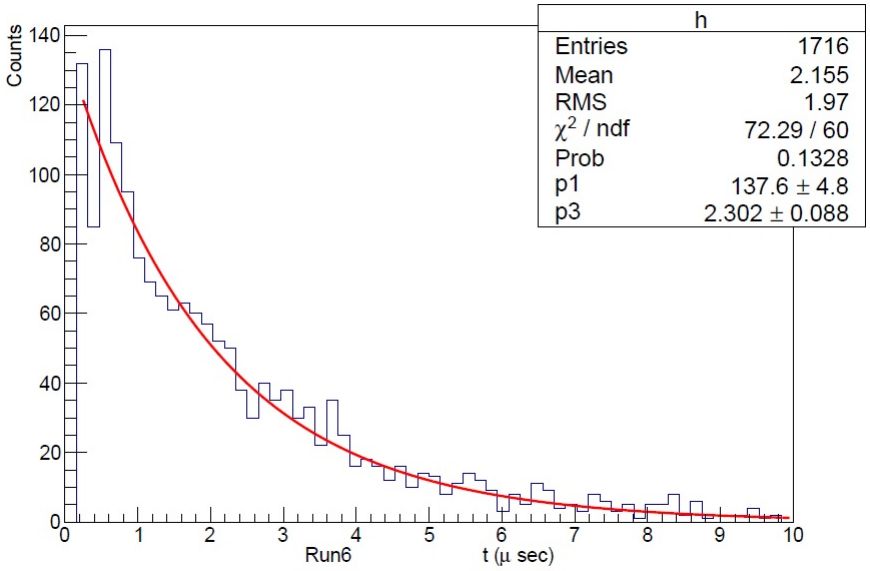

Figure 3.12: The histogram obtained for the final muon lifetime experimental run.

The relation of the activity of a radioactive source to time is given by $A(t) = Ae^{-t\Gamma}$. Here Γ is the decay rate and this is a universal law for all radioactive sources which decay. And it applies to muons. The histograms, obtained from the MCA data, had the general from of decaying exponential function. When the histograms were fitted with the function given by the equation 3.4 we got the value of τ one for that experimental run.

Data was then taken from the MCA software and analysed using ROOT [6]. The programme took the raw MCA data, constructed the histogram, converted the channel scale to time scale and then fitted the histogram with the exponential function:

$$f(t) = C(0.44e^{-\frac{t}{1.7}} + 0.56e^{\frac{t}{\tau}}) \tag{3.4}$$

After fitting the histogram the programme returned to us the values of C and τ.

In equation 3.4 the first term corresponds to μ^- and the second to μ^+. Their two respective weights of 0.44 and 0.56 were taken from the muon charge ratio R which was shown earlier in this report [4]. The value of the mean lifetime that we eventually got was:

$$\tau = 2.30 \pm 0.09 \mu s$$

Here ± 0.09 is the statistical uncertainty in our value. The actual value of the mean lifetime of the muon is within 2σ of our measured value.

Chapter 4

Measuring the Muon Velocity

4.1 The Experiment

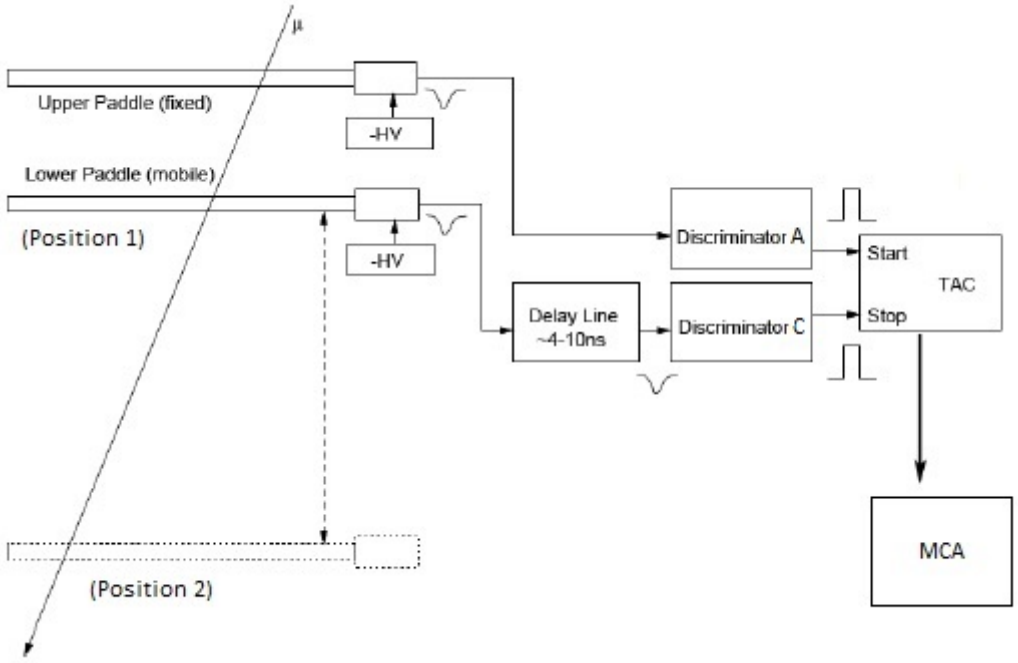

Figure 4.1: The basic experimental setup of the muon velocity experiment [4].

In this experiment the time taken for the muon to pass between two points was measured and by measuring the distance between these points it was possible to estimate the velocity of the muon.

The setup is shown in Figure 4.1. Pulses from detector A were fed into the START input of the TAC and pulses from C to the STOP input of TAC. The time range of the TAC was moved to its minimum range which was 0-50 ns. Now a time range of 0-50 ns corresponded to voltage range of 0-10 V for pulses generated by the TAC. The time range was shortened because the time taken by the muon to travel a distance of 4 m (roughly the maximum vertical distance available to us in our lab) at a predicted speed of around $0.98c$ was around 13.6 ns. Therefore to optimise the resolution of our

MCA spectrum the time range was decreased. The resolution of our MCA spectrum therefore now became 50 ns/8192 channel=0.0061 ns/channel.

The pulse of PMT C had to be delayed so that the expected Gaussian spectrum of the time taken by the muon, to traverse from A to C, is well within our $50ns$ MCA spectrum time scale and does not get cut from its from its edges. The amount of delay depended on how much we wanted to shift our Gaussian time curve towards the right on our time scale on the MCA spectrum so that the curve is fully displayed on the spectrum.

4.2 Initial runs

In our initial runs voltages of PMTs A and C were kept at 1100 V each and the discriminator thresholds were kept at -50 mV each for A and C. A delay of approximately 10 ns was introduced by having 3 limo cables, joined by two limo barrels, between the discriminator output and the STOP input of TAC. The data received was analysed using ROOT and was fit with a Gaussian model [6]. The fitted histograms of both the runs are shown in Figure 4.2 and Figure 4.3. The experiments were generally run for around $10,000$ s. Some typical results of fitted histograms are shown in Figures 4.2 and 4.3. The advantage of the delay can be seen in these figures that the Gaussian peaks that we got are within our MCA spectrum and did not get cut from the sides.

A time distribution was obtained for two different positions of the detectors which gave us two equations for each of our run.

$$D_1 = v_\mu t_1 \text{ and } D_2 = v_\mu t_2$$

Here t_1 and t_2 are the mean values of time taken by muon to travel between the detectors and were given to us by the mean values of both Gaussian curves. It should be also realised that time also contains the factor of delay which was introduced to shift the Gaussian curve on our MCA. D_1 and D_2 are values of distance for each of the respective runs.

Subtracting both these equations eliminates the factor of delay and gives us [4]:

$$\triangle D = v_\mu \triangle t$$

4.3 Calculating the value of average distance travelled by muon

The angular distribution of the incident muon flux at a certain altitude is given by [4]:

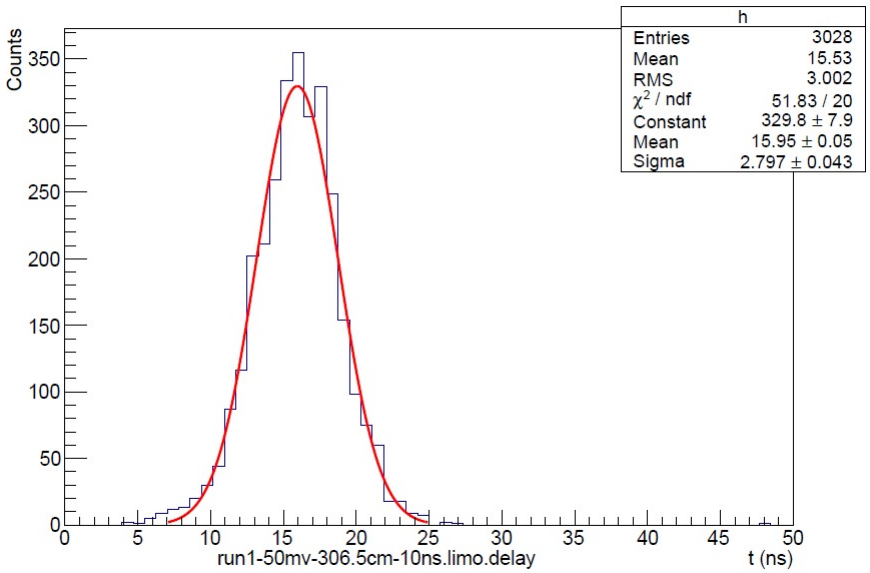

Figure 4.2: The histogram obtained with 306.5 ± 1.0 cm distance between the detectors.

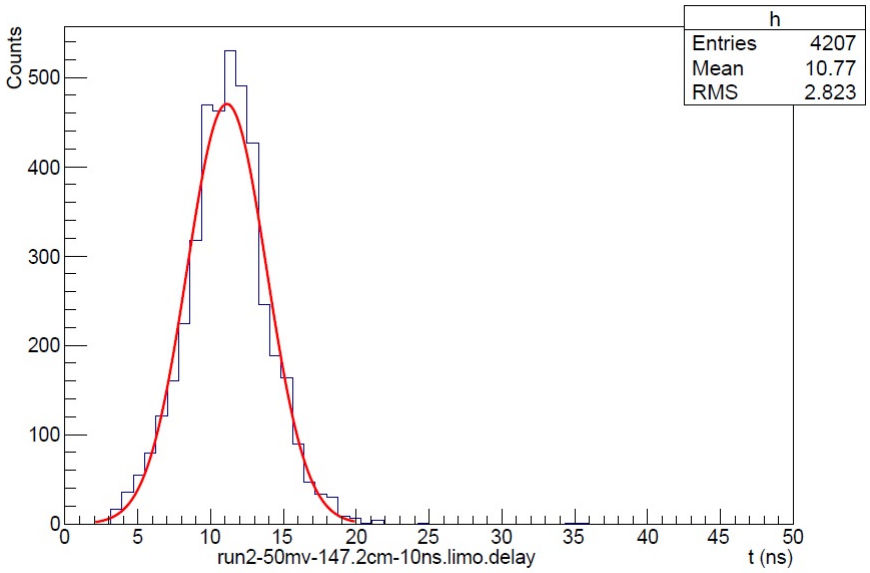

Figure 4.3: The histogram obtained with 147.2 ± 1.0 cm distance between the detectors.

$$I(\theta) \propto \cos^2(\theta) \tag{4.1}$$

This means that most of the muons are incident normally on the detectors but still they can come from any θ. Although the flux of the incident muons decreases with increasing angle. To calculate the average distance travelled by muons through the detectors a Monte Carlo simulation was performed as described below.

In each muon event in the simulation, as shown in Figure 4.4, a muon was first assigned random values of θ, ϕ, x_i and y_i. θ as shown in Figure 4.4 is the angle measured from the vertical. For x_i, y_i and ϕ we chose uniform probability distribution functions but for θ a probability distribution function of $\cos^2\theta$ was chosen. This represents the

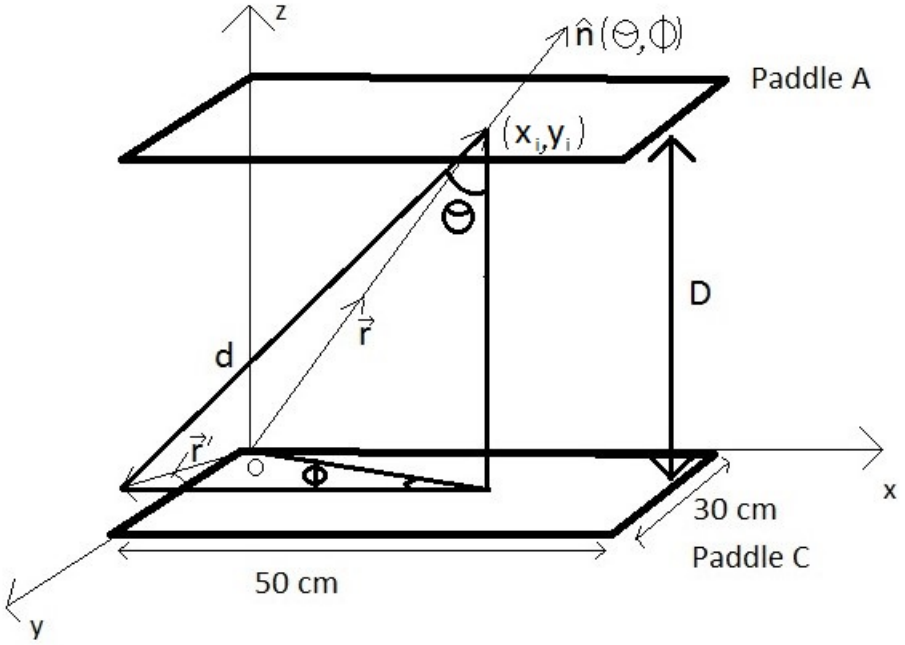

Figure 4.4: The geometrical setup for the Monte Carlo simulation for the trajectory of the muons.

variation of the flux of muons with θ as inferred from the $\cos\theta$ term in equation 1.2 which was shown earlier and also from the fact that intensity of muons varies with $\cos^2\theta$. The initial x_i and y_i coordinates assigned to the muon gave the hit position in the plane of upper detector A and θ and ϕ assigned to the muon gave us the trajectory of the muon for that particular event.

The final x and y coordinates were calculated when the muon had traversed the vertical distance D and its z-coordinate was equal to zero . This was done using simple vector subtraction. We defined three vectors as shown in Figure 4.4, which were $\vec{r}$, $\vec{r}$ and $\hat{n}$. $\vec{r}$ was the position vector of the starting point of the muon, $\vec{r}$ was the position vector of the final position of the muon at $z = 0$ and $\hat{n}$ is a unit vector opposite to the direction followed by the incident muon. The final position coordinates of the muons were determined by solving the following vector equation:

$$\vec{r} = \vec{r} - d\hat{n} \tag{4.2}$$

Here the d is the distance of the path travelled by the muon in the vertical height D. If the final coordinates of the muon x_f and y_f lied within the rectangular paddle C then the event was considered as a HIT and if the final coordinates lied outside the paddle C then the event was considered a $MISS$ and the value of d was discarded.

The simulation was run for one million events. Out of those 312182 were HITs and rest were a $MISS$. Figures 4.5, 4.6, 4.7, 4.17 and 4.10 show the results which were obtained from the simulation for distance D of 436.9 cm . These figures only show the distributions obtained from the HITs. Figure 4.5 shows the distribution of d. As it can be seen the mean value of d is 437.2 cm which is very close to the actual value of the D. However if we decreased the value of D to around $200cm$ in the simulation then mean value of d obtained was 200.7 cm. Therefore this clearly showed that at

short distances the mean of value d deviated by a greater percentage from the value of D than at large distances i.e. large values of D. The resulting z distribution ensured the simulation was working correctly by giving all the x y coordinates on Paddle C a z coordinate of 0 which is actually how the simulation was built up.

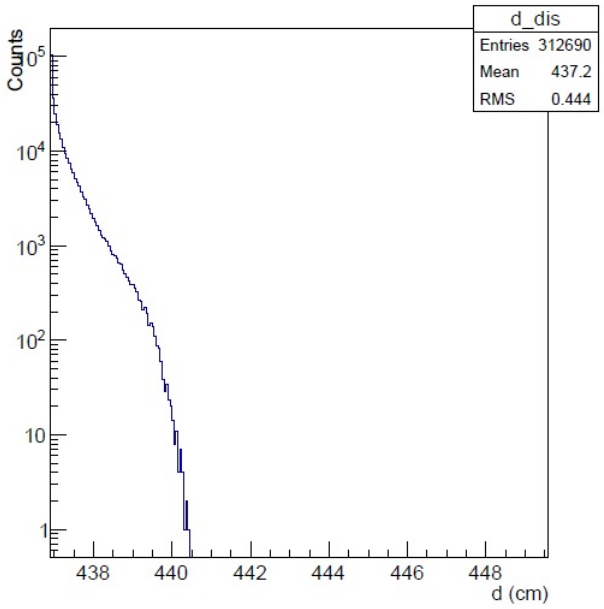

Figure 4.5: This figure shows the distribution of d as generated by the simulation. This is for $D = 436.9$ cm.

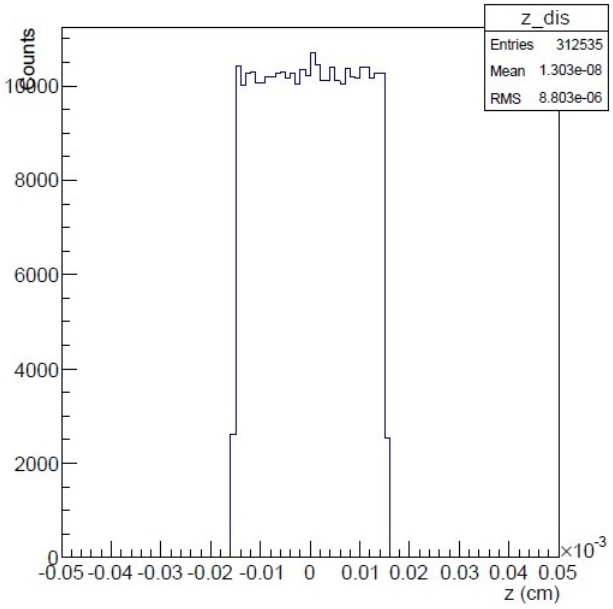

Figure 4.6: This figure shows the distribution of z as generated by the simulation.

Figure 4.7 also shows the distribution of θ of the incident muons. As it can be clearly seen most of the muons were incident at small angles to the vertical.

We obtained the average distance traversed by a muon passing through the two detectors. From this the time taken for the muon to travel from A to C, t_{AC}, could also be calculated. The velocity of the muon in air was assumed to be $v_\mu = 2.98 \times 10^8 ms^{-1}$ [4]. And with knowledge of the refractive index of the plastic material we could also

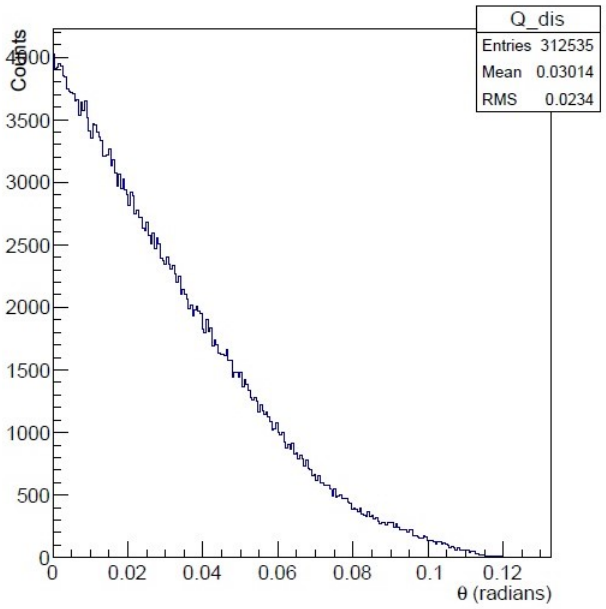

Figure 4.7: This figure shows the distribution of θ as generated by the simulation.

calculate the time taken by light to travel from the point of the incident muon to the detector. For both the paddles this time was labelled as t_A and t_C. The advantage of calculating these times and deviations was that it could give us an idea of the spread that we should have in our Gaussian peak being observed in the MCA. Our results from the simulation would then be comparable with our experimental results.

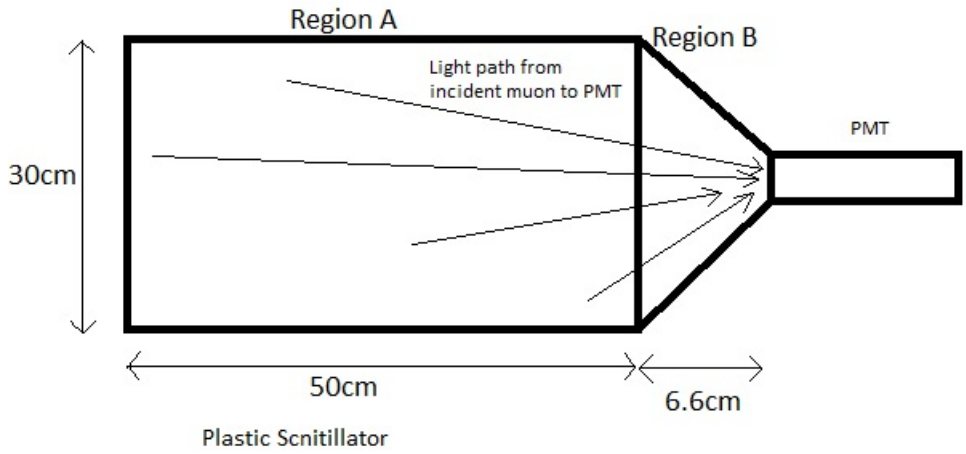

Figure 4.8: The possible paths of light from point of incident muons to the PMT. The times t_A and t_C were calculated using this distance and velocity of light in Polyvinyl toluene muons were only assumed to hit in Region A of the scintillator and not in Region B. However the 6.6 cm distance was included in the path that light had to travel to get to the PMT.

The refractive index of polyvinyl toluene as mentioned earlier is $n = 1.58$ and from $v = c/n$ the velocity of light in the plastic was calculated. Then using the simulation

the distance from the incident point to the PMT was calculated as shown in Figure 4.8. Then using the velocity and distance values of t_A and t_C were calculated.

For calculating t_{AC} the velocity of muon was assumed to be $2.98 \times 10^8 ms^{-1}$ [4]. The distance travelled by the muon between the two paddles was given by the distribution of d. Using these values the distribution of t_{AC} was found out.

The time interval that we were measuring on the MCA is explained with the help of Figure 4.9. When the muon hits and crosses the paddle A it emits light which takes time t_A to reach the PMT. After that time t_A our electronics receive the first pulse. In that time t_A the muon also moves a distance d_A on its way to paddle C as shown in the Figure 4.9. Then it further moves a distance $\acute{d}$ after which it hits paddle C. When it hits paddle C it emits light which reaches the PMT in time t_C. So essentially the time interval we were measuring on the MCA was the time:

$$\Delta t_{MCA} = \frac{\acute{d}}{v_\mu} + t_C$$

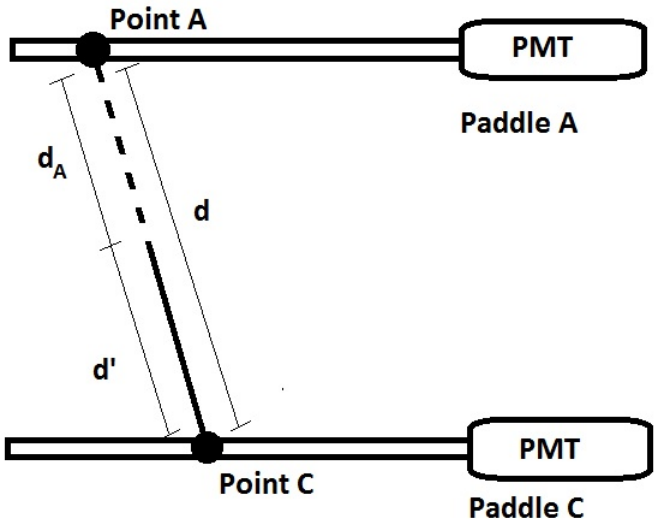

Figure 4.9: This figure shows the a general path of the muon between detectors A and C and helps in explaining the interval being measured by us on the MCA.

The time interval measured or Δt_{MCA} was different from the time t_{AC} which was the actual time taken by the muon to travel from Paddle A to Paddle C. The distributions of t_A, t_C, t_{AC} and Δt_{MCA} or time measured are shown in Figure 4.17. All these results are for $D = 436.9cm$. It can be seen that the mean of t_{AC} is slightly smaller than the Δt_{MCA} mean. This shows that there was small inherent delay caused by the experimental setup in the time t_{AC}, of around ~ 2 ns in this case. However this distribution did give us an idea of the actual contribution of these times to our overall experimental MCA spectrum.

One interesting result that was obtained from these time distributions was t_A was plotted against t_C as shown in Figure 4.10. As we can see most the counts lie on the straight line and t_A and t_C have a linear relationship and are directly proportional. This meant that most of muons were incident normally on the detectors.

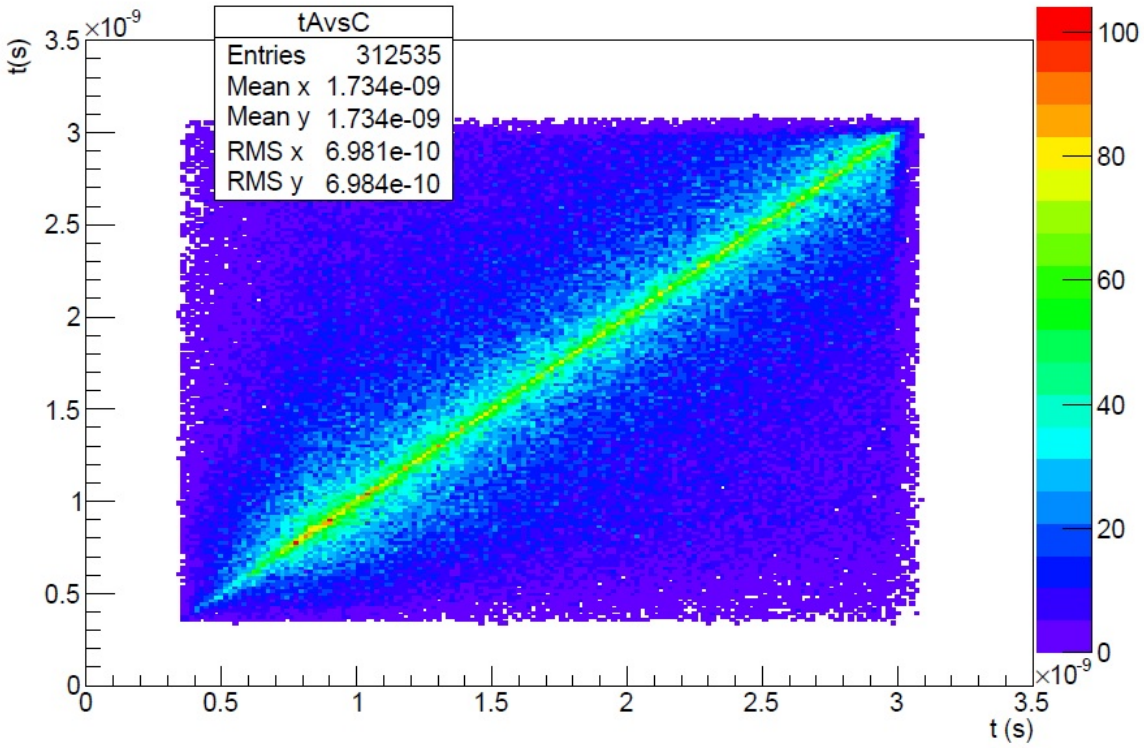

Figure 4.10: The figure shows t_A plotted against t_C. The straight line shows that they have a linear relation.

4.4 Predicting the flux through detectors A and C.

Detector A was placed such that the vertical distance, D, between A and C was $436.9cm \pm 0.5cm$. To check that our detectors were working as expected we decided to take a run of the muon lifetime experiment by keeping the detector B between these two detectors. Detector B was placed such that its distance from A was $245.6 \pm 0.5cm$ and its distance from C was $191.3 \pm 0.5cm$.

When the muon lifetime experiment was started it was noticed that the coincidence rate of AB$\bar{\text{C}}$ and B2 dropped to a really low value around 1 count for every 5 minutes. This had been expected however such a low coincidence rate meant that the experiment would have to be run for a really long time to gain enough data so as to reduce the amount of statistical error.

As there was not that much time available to us we decided to measure the coincidence rate of detectors B and C at different positions. Detector B was kept fixed in its own position and the position of detector C was varied. This data would then be used to predict the coincidence rate of detector B and A at their given positions. A was not moved as it was kept extremely high and moving it would have been a risky and clumsy process.

Pulses from detectors B and C were passed through their respective discriminator units and using logic units BC coincidence pulse was generated. The logic unit was

kept at coincidence level 2. One pulse output from the logic unit was taken and connected to the START input of the TAC. A 2nd input from the logic unit was taken delayed a little using a delay unit on the Quad delay generator. And then the output of the delay unit was connected the STOP input of the TAC.

Each pulse from the TAC represented a BC coincidence pulse. As the delay was fixed all the pulses generated by the TAC were a of a fixed height and generated a single peak on the MCA channel spectrum. This experiment was carried out 7 times each time at a different position of C. Each run was carried out for a time interval of $300s$. The following table shows the different positions at which detector C was kept:

Run no.	Distance between B and C ($\pm$0.5 cm)
1	191.3
2	159.5
3	126.9
4	96.2
5	36.4
6	23.3

Our aim was to plot a graph of number of BC pulse counts against the distance between the detectors B and C. We were expecting a $1/r^2$ distribution as intensity varies in such a way. The resulting curve that we got is shown in Figure 4.11.

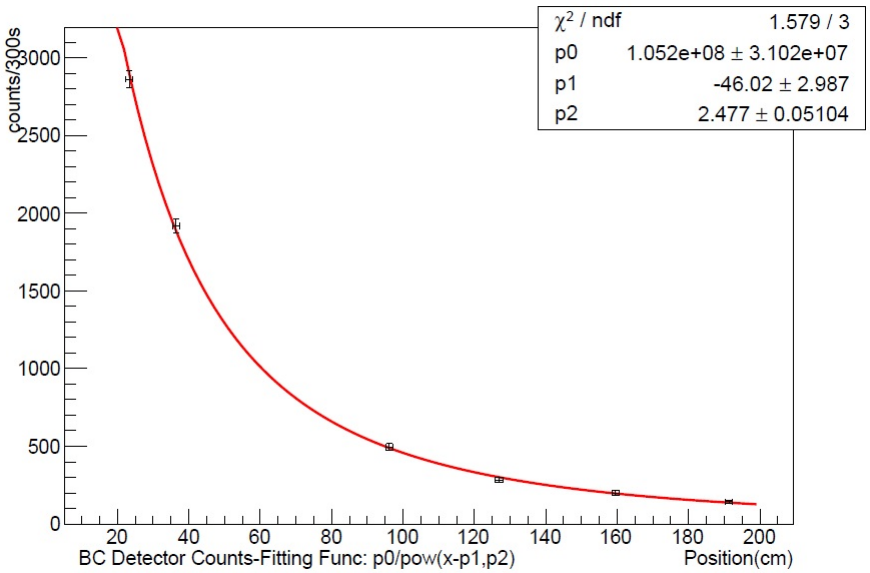

Figure 4.11: The graph shows No. of BC Counts against distance between both the detectors.

The curve in Figure 4.11 was fitted using the function $N = \frac{a}{(r-b)^c}$. Here N is the number of counts of BC and r is the distance between the two detectors. a, b and c are fitting parameters and their values were given by:

$$a = (1.05 \pm 0.31) \times 10^8 cm^2$$
$$b = -46 \pm 3cm$$
$$c = 2.48 \pm 0.05$$

A was at a distance of $245.6 \pm 0.5cm$ from detector B. Using our fitting function it was predicted that in a period of 300 s at this distance of detectors A and B their coincidence would generate around ~ 83. Experimentally we carried out this process and got 93 counts for AB coincidence in 300 s. These answers were close to each other to a sufficient degree and showed that our detectors in their respective positions were working as expected.

4.5 Final Runs

Finally it was decided to run the velocity experiment again. In the first experimental run the delay in the pulse of detector C was of 24 ns and was introduced using the delay box. The delay box is an electronically passive device and therefore it was expected that it would not generate any electronic noise. The distance D between the detectors was varied 4 times for each experimental run. A was kept in its fixed position while the position of C was varied. The following table shows the the distances between A and C for each of the four positions:

Run no.	D_{AC} ($\pm$0.5 cm)
1	436.9
2	372.5
3	311.4
4	241.4

Here D_{AC} is the vertical distance between the center of the two detectors, A and C.

The threshold of both of the discriminator units was kept at -50 mV and the voltage of both the PMTs was fixed at 1100 V. These two parameters were kept constant for all runs. After obtaining data from the MCA for the data was plotted for each position giving us the Gaussian-like histogram. The histogram was fitted with a Gaussian function and using the fit a mean value of Δt was obtained. For each position the mean value of d was obtained from the simulation. The values of d_{mean} and Δt, given by the table below, were then plotted against each other to give us a D vs T graph. The slope of this graph then gave us the speed of muon, v_μ.

Table 4.1: Run 1 values

Run no.	d_{mean} ($\pm$0.5 cm)	Δt_{avg} (ns)
1	437.2	35.76 ± 0.05
2	372.9	33.72 ± 0.03
3	311.8	31.82 ± 0.04
4	242.0	29.72 ± 0.03

Results for the first run are shown in Figure 4.12.

The velocity of muon obtained from run 1 was $v_\mu = (3.25 \pm 0.3) \times 10^8 ms^{-1}$.

In the the second run the delay was increased to 56 ns using the delay box and the time scale of the TAC was increased to 100 ns. It was suspected that at its smallest

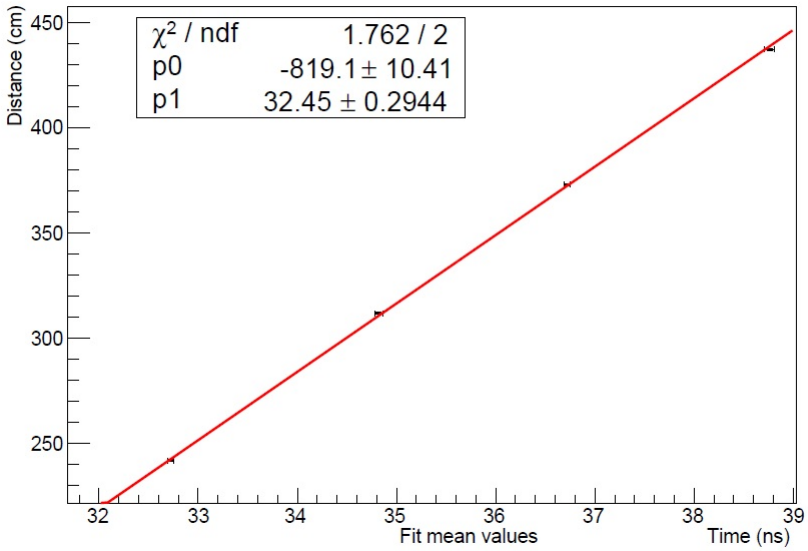

Figure 4.12: D vs T graph for run 1 of the final runs of the velocity experiment.

time scale of 50 ns the TAC might have been acting non linearly causing a systematic error in our velocity value. In order to check that whether this was actually the case the scale was changed by increasing it to 100 ns. The rest of the parameters remained unchanged. Results of run 2 are shown by Figure 4.13. The values of d_{mean} and Δt plotted in Figure 4.13 are given in the table 2.

Table 4.2: Run 2 values

Run no.	d_{mean} ($\pm$0.5 cm)	Δt_{avg} (ns)
1	437.2	65.78 $\pm$ 0.06
2	372.9	63.71 $\pm$ 0.05
3	311.8	61.75 $\pm$ 0.04
4	242.0	59.67 $\pm$ 0.04

The velocity of muon obtained from run 2 was $v_\mu = (3.20 \pm 0.4) \times 10^8 ms^{-1}$. The value of velocity did not change as compared to the previous run, the error range increased and still our value was beyond the limit of speed of light.

Then for our third run positions of detectors A and C were swapped with each other. Now positions of detector A were varied while detector C was kept fixed at its point. Previously detector A had been the detector which was placed above the C detector but now detector C was above detector A. Both the detectors were identical and swapping their places should not have affected our value for velocity of muon in any way. Results of the run 3, shown by Figure 4.14, told us a different story. The TAC time scale in this run was reduced back to 50 ns and the delay in the A pulse was of 24 ns using the delay box. All of the other parameters were not changed. The values of d_{mean} and Δt plotted in Figure 4.14 are given in the table 3.

The velocity of muon obtained from run 3 was $v_\mu = (3.16 \pm 0.3) \times 10^8 ms^{-1}$. As can be clearly seen the value of the velocity did decrease however not sufficiently enough

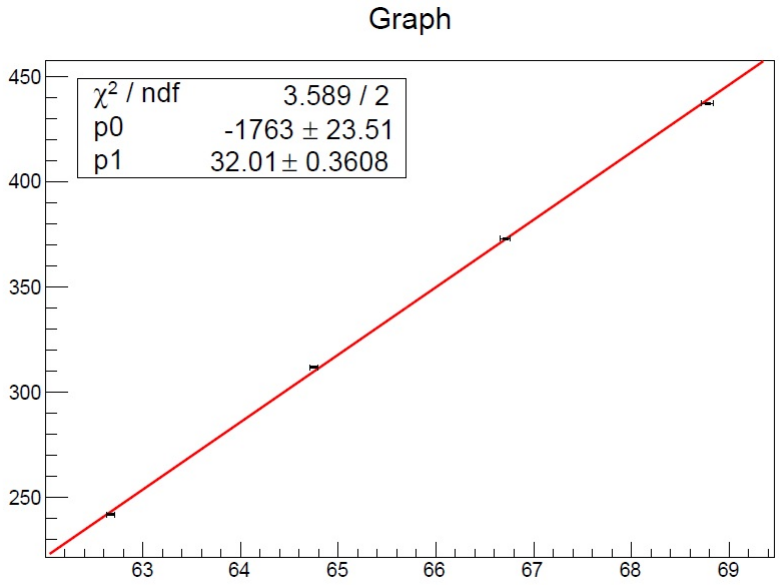

Figure 4.13: D vs T graph for run 2 of the final runs of the velocity experiment.

Table 4.3: Run 3 values

Run no.	d_{mean} ($\pm$0.5 cm)	Δt_{avg} (ns)
1	437.2	35.25 $\pm$ 0.04
2	372.9	33.18 $\pm$ 0.04
3	311.8	31.31 $\pm$ 0.05
4	242.0	29.07 $\pm$ 0.03

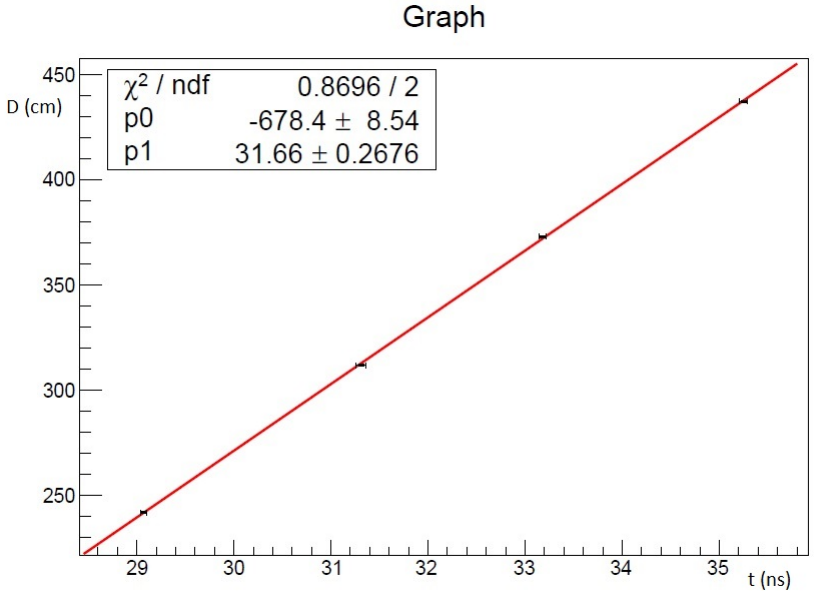

Figure 4.14: D vs T graph for run 3 of the final runs of the velocity experiment.

to give us the correct answer. It also proved that both detectors A and C had some

internal dissimilarities and were not functioning in the same way.

To check whether it was actually the case, that both the detectors A and C were not working in the same way, both the detectors were kept on top of each other with a 2 cm distance between them. And data was recorded on the MCA for a time interval of around 450 s. First detector A was kept on top of C and data was acquired and then detector C was swapped with A by keeping it on top of A and then the data was again acquired. In both the cases the delay was kept to 24 ns and TAC time scale was kept at 50 ns. The two spectrums obtained from the MCA are shown by the Figures 4.15 and 4.16.

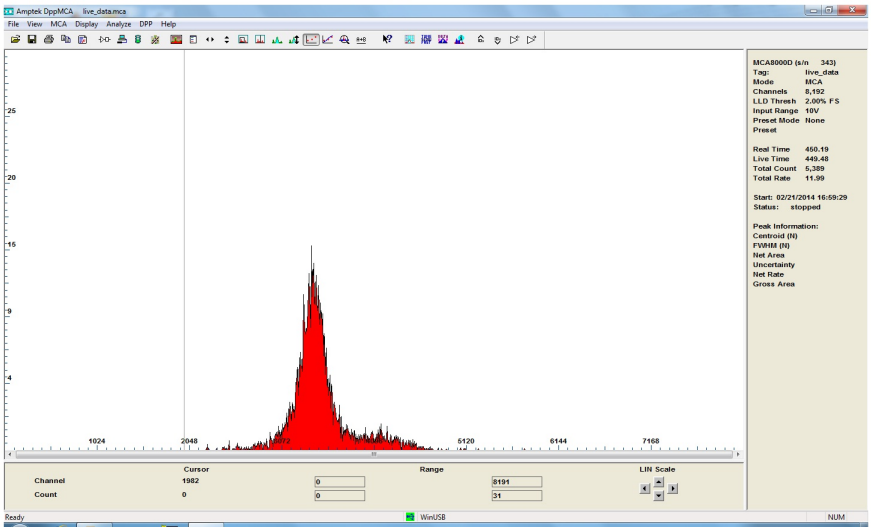

Figure 4.15: MCA spectrum for A on top of C.

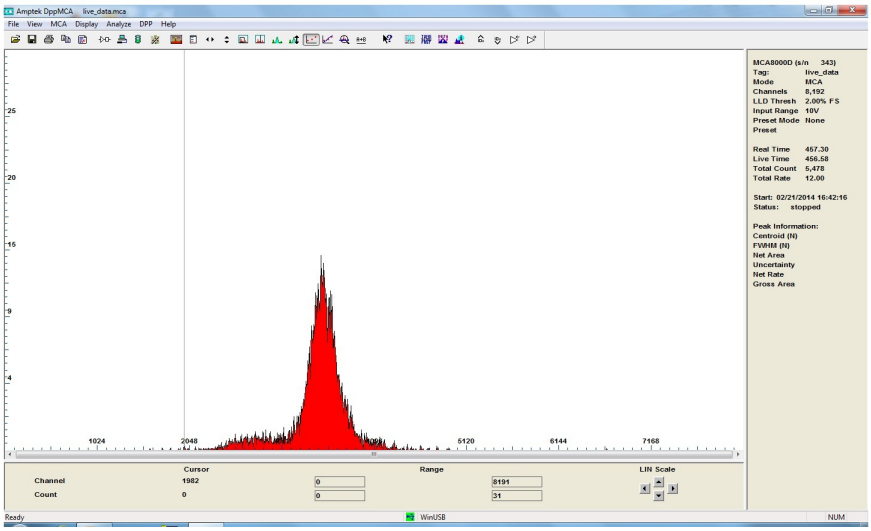

Figure 4.16: MCA spectrum for C on top of A.

As it is very apparent from these two spectrums both the detectors have a very different curve. This could have been a possible source of error in our velocity readings. It can also be the discriminator units being used in this experiment.

Our final average muon velocity was:

$$< v_\mu >= (3.2 \pm 0.1_{sys} \pm 0.3_{stat}) \times 10^8 ms^{-1}$$

This value was within 2σ of the expected value of v_μ. Here 0.3 is the statistical error and 0.1 is a conservative estimate of the systematic error in the value.

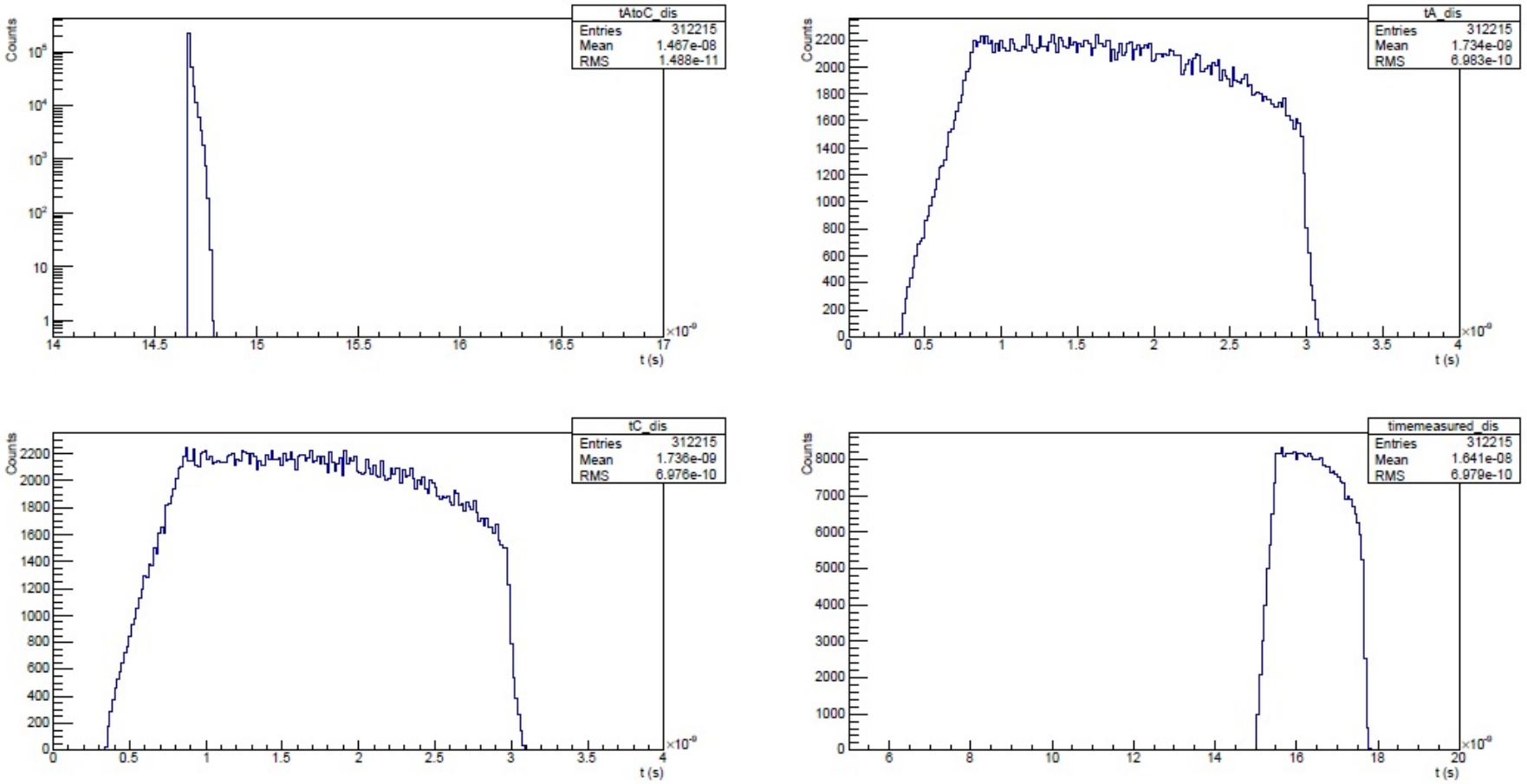

Figure 4.17: This figure shows the distributions of *timemeasured* or Δt_{MCA}, t_A, t_C and t_{AC} which were generated by the simulation.

Chapter 5

Conclusion

The muon lifetime experiment gave us very good results and now can be properly setup and be assigned to undergraduate students who can learn of data analysis from it and can also learn about basic principles experimental particle physics. Although we were not able to get the proper muon velocity but we were very close to it. The experiment is now being improved by building a lift for detector A such that detector C will remain stationary and the position of detector A will be varied. The lift would allow us take readings from multiple positions and more readings would help refine our D vs T. Constant Fraction discriminators, which were not used in this experiment, might also be able to help us improve our velocity readings

5.1 Acknowledgements

I would like to thank my supervisor Dr. Imran Younas for his guidance and help throughout these two experiments and also like to thank my professor Dr. Sabieh Anwar for his guidance and support.

Bibliography

[1] Stanev; Todor, "*High Energy Cosmic Rays*", Springer, 2010 and the references therein.

[2] Universidad Nacional de La Plata, April 25th 2014, Muon Basics, http://www2.fisica.unlp.edu.ar/ veiga/experiments.html

[3] "*Lifetime of the Muon*", NP08, Oxford Physics, Particle Physics Projects Manual, revised MGB Oct 2006.

[4] Liu, Lulu; Solis, Pablo , "*The Speed and Lifetime of Cosmic Ray Muons*", MIT Undergraduate Experiment report, Nov 18, 2007. and the references therein.

[5] http://www.rexon.com/

[6] http://root.cern.ch/drupal/